

A general theory of differentiated multicellularity

Felipe A. Veloso¹✉

¹Faculty of Biological Sciences, Universidad Andrés Bello, Santiago, Chile

✉Correspondence: veloso.felipe.a@gmail.com

Abstract

There is wide scientific consensus on the relevance of changes in the levels of gene expression for the cell differentiation process. Furthermore, research in the field has customarily assumed that such changes regulate this process when they interconnect in space and time by means of complex epigenetic mechanisms. Nevertheless, this assumed regulatory power lacks a clear definition and may even lead to logical inconsistencies. To tackle this problem, I analyzed publicly available high-throughput data of histone H3 post-translational modifications and mRNA abundance for different *Homo sapiens*, *Mus musculus*, and *Drosophila melanogaster* cell samples. Comprising genomic regions adjacent to transcription start sites, this analysis generated for each cell dataset a profile from pairwise partial correlations between histone modifications controlling for the respective mRNA levels. Here I report that these profiles, while explicitly uncorrelated to transcript abundance by construction, associate strongly with cell differentiation states. This association is not to be expected if cell differentiation is, in effect, regulated by epigenetic changes in gene expression. Based on these results, I propose in this paper a falsifiable theory of differentiated multicellularity. This theory describes how the differentiated multicellular organism—understood as an intrinsic, higher-order, self-sufficient, self-repairing, self-replicating, and self-regulating dynamical constraint—emerges from proliferating undifferentiated cells. If it survives falsification tests consistently this theory would explain in principle (i) the self-regulated gene transcriptional changes during cell differentiation and (ii) the emergence of differentiated multicellular lineages throughout evolution.

26 Introduction

27 The X-files of chromatin

28 Cell differentiation, if seen as a motion picture in fast-forward, intuitively appears to be a
29 teleological process, its *telos*¹ being the multicellular organism in its mature form. The first step
30 for a scientific explanation of this apparent property was given in 1957 when Conrad Waddington
31 proposed his epigenetic landscape model. Influenced by earlier developments in dynamical
32 systems theory [1], Waddington's model showed cell differentiation to be potentially predictable
33 or at least potentially explainable without any teleological reference [2].

34 In terms of explainability, the dynamics of the cell differentiation process have been associated
35 to changes in chromatin states and concurrent heritable changes in gene expression that are
36 explicitly uncorrelated to changes in the DNA sequence (for this reason defined as epigenetic
37 changes [3, 4]). In some cases these changes can be regulated extrinsically with respect to the
38 developing organism, as observable in eusocial insects (e.g. a female honeybee larva develops into
39 a worker or a queen depending on the royal jelly diet it is fed [5]). Nevertheless, most key changes
40 in gene expression during cell differentiation are not only independent from, but are even robust
41 with respect to extrinsic variables. This means cell differentiation is fundamentally an intrinsically
42 regulated process, for which no falsifiable theory has emerged from the epigenetic framework
43 since it was first advanced. Moreover, Peter Fraser has recently referred to this problem as
44 “The X-files of chromatin” [6].

45 This research work was conceived and designed to, following Fraser's metaphor, declassify
46 “The X-files of chromatin”. In its initial phase, I conducted a computational analysis of the least
47 relevant—for the epigenetic landscape—constraints on histone H3 post-translational modification
48 states. Before outlining this analysis however, I must present here a case for the fundamental
49 impossibility of explaining the cell differentiation self-regulatory dynamics under the framework
50 pioneered by Waddington, however complex its underlying mechanisms may be (as also hinted
51 by Fraser [6]). Only then will I be able to argue that these epigenetically irrelevant constraints on
52 histone modification states are, in fact, key to a full understanding of differentiated multicellularity
53 in terms of its self-regulation and evolution.

54 The conundrum of self-regulation

55 Avoiding non-explanatory teleological descriptions, modern science regards cell differentiation
56 fundamentally as a dynamical system, where a fixed rule governs the transition between the
57 realizable states of a complex network of molecular mechanisms. Ranging from low-order
58 molecular interactions [7] to chromatin higher-order structural changes [8, 9], these epigenetic
59 mechanisms not only propagate changes in gene expression in different loci as cells proliferate
60 but, importantly, would also *regulate* intrinsically the cell differentiation process. Furthermore,
61 and although the epigenetic mechanisms involved in cell differentiation are far from being

¹τέλος is the Greek for “end”, “goal”, or “purpose”.

62 completely elucidated, the hypothesis that cell differentiation is *regulated* by heritable changes
63 in gene expression is routinely presented to the general public as a well-established scientific
64 fact (as illustrated in [10]). However, this hypothesis—whether or not we accept it in its strict
65 sense—leads to severe explanatory limitations and may even entail logical inconsistencies.

66 To assume the aforementioned hypothesis is true in its strict sense is to accept gene self-regulation
67 as a scientifically tenable and explainable teleological property of cell differentiation (the “intuitive”
68 *telos* here would be certain future transcriptional states to be timely achieved or maintained).
69 To explore what this implies let us suppose, for simplicity without loss of generality, that a
70 researcher modifies the expression levels of certain *geneA* in certain organism and then elucidates
71 how those changes, during differentiation, activate or repress *geneB*, *geneC*, and *geneD*. At this
72 point, we might regard the finding as evidence that *geneB*, *geneC*, and *geneD* are regulated
73 by *geneA*. Consequently, we could also hold that *geneA* is an explanatory component of the
74 general self-regulatory property. However, these assertions overlook that the researcher, not
75 *geneA*, was the true regulator by purposefully imposing certain transcriptional states (on *geneA*,
76 and by means of *geneA*, also *geneB*, *geneC*, and *geneD*). Yet, no human regulator is needed during
77 the natural process, which raises the question of what is the system truly regulating *geneA*, *geneB*,
78 *geneC*, *geneD*, and by extension, all genes during cell differentiation.

79 Moreover, explaining the regulation of transcriptional states in a gene locus by previous
80 transcriptional states in other gene loci (in the same cell or any other) is only a non-explanatory
81 regress. It takes the question about regulation, i.e. explaining a gene being at certain
82 transcriptional states (and, importantly, at no other transcriptional states), to some other gene
83 or genes, back in time. This regress inexorably leads—even in the simplest scenario—to the
84 unexplained, timely regulation of one key gene (or more key genes, simultaneously) within
85 undifferentiated cells.

86 On the other hand, to take the epigenetic-changes-regulate hypothesis in a loose sense is to use
87 “self-regulation” only as a placeholder when referring to a certain class of molecular mechanisms
88 *propagating* changes in gene expression. In this context we must note that a defining condition
89 of any mechanism is that the changes it comprises are *explicitly correlated*. Thus, an epigenetic
90 mechanism can be seen metaphorically as toppling dominoes (here the explicitly correlated
91 changes are obvious). But as pointed out previously this mechanism, however numerous or
92 intricately connected its correlated changes, says nothing about how the first domino tile (or
93 any other whose fall is not attributable to the fall of other tiles) was toppled over. To fill this
94 explanatory gap, it has been proposed that an “epigenator”—defined operationally as a transient
95 signal which probably originates in the environment of the cell—triggers the epigenetic phenotype
96 change after being transduced into the intracellular space [11]. Nonetheless, if all “epigenators” in
97 the developing organism are extrinsic to it, self-regulation is *ipso facto* unexplainable. Otherwise
98 if there is at least one intrinsic “epigenator” (e.g. a suggested “extracellular signal”) its critical
99 signaling property is left unexplained.

100 Importantly, these problems are inherent to *any* model based on Waddington's epigenetic
101 landscape. This is because *the changes in any mechanism regulating changes in gene expression*
102 *must be explicitly uncorrelated to the those changes; otherwise this mechanism is, fundamentally, just*
103 *an "additional set of arranged domino tiles" propagating gene expression changes more extensively*
104 *instead of regulating them* (see [Figure 1A](#)). At this point the explanatory dead end becomes
105 evident. Under the traditional approach in developmental biology no higher-order system within
106 a living organism, however complex (e.g. displaying interlocked feedback loops or hypercyclic
107 networks), can exert true intrinsic regulation because its dynamics are ultimately correlated to
108 the lower-order dynamics it is supposed to regulate. Thus, the supposed *regulatory* power of
109 changes in gene expression on the cell differentiation process is causally inefficacious in the most
110 fundamental sense.

111 Progress comes from recognizing that the propagation of critical changes within a developing
112 organism and the intrinsic regulation of such changes are entirely different processes. Specifically,
113 intrinsic regulation is not a molecular mechanism—however complex—correlating the levels of
114 critical variables within a developing organism but instead *constraints* on the realizable levels
115 of said variables. Importantly, these constraints must be also *explicitly uncorrelated* to regulated
116 levels as argued previously.

117 **Epigenetic information in theory and practice**

118 Regardless of the explanatory limitations inherent to the epigenetic landscape, either all necessary
119 information for the intrinsic regulation of cell differentiation is already contained in the zygote
120 or the spore or it is not. This dichotomy may seem to be trivial but important implications
121 follow it.

122 If the zygote or spore contains all necessary information for intrinsic regulation [12, 13],
123 the previously discussed explanatory gap could, in principle, be filled. Asymmetric early
124 cleavage, shown able to resolve a few commitments (into six founder cells) in the nematode
125 *Caenorhabditis elegans* [14], supports this possibility at first glance. Nevertheless, a closer look at
126 the developmental complexity of this simple metazoan model organism suggests otherwise: the
127 hermaphrodite *C. elegans* ontogeny yields 19 different cell types (excluding the germ line) in a total
128 of 1,090 generated cells. From these two parameters alone, the required information capacity for
129 the entire process can be estimated to be at least 983 bit (see details in the [Appendix](#)). Further,
130 this is a great underestimation since cell-fate uncertainty remains with respect two more variables
131 at least, namely space and time. Therefore, the non-genetic information capacity necessary for
132 the entire process far exceeds the few bits of information that epigenetic mechanisms (even if
133 asymmetric early cleavage is entirely explained by them) can account for. On the other hand,
134 the explanatory power of extrinsic constraints (e.g. diet-dependent hierarchy determination
135 in eusocial insects [5], temperature-dependent sex determination in reptiles [15], or maternal
136 regulation of offspring development [16]) is clearly unable to account for all developmental
137 decisions and in some cases it is not even indispensable. These considerations highlight
138 the remarkable explanatory power of certain *intrinsic* constraints—to be identified here—on
139 developmental decisions in terms of information capacity.

140 Information not only requires a medium with capacity for its storage and transmission but also
141 must have content, which resolves developmental decisions as cells proliferate. Here an additional
142 problem appears: cell potency. An entire organism can develop (including extraembryonic tissues)
143 from *any* totipotent cell, and all embryonic tissues can develop from *any* pluripotent stem cell.
144 How is this possible if the information for all cell fate decisions is already contained in the
145 zygote or the spore? The recently proposed—yet not explanatory—“epigenetic disc” model for
146 cell differentiation, under which the pluripotent state is only one among many metastable and
147 directly interconvertible states [17], reflects the necessity to account for the context-dependent
148 character of developmental information.

149 With remarkable insight, David L. Nanney anticipated in 1958 explanatory pitfalls if the definition
150 of epigenetics is limited to heritable changes. He further stated that “‘cellular memory’ is
151 not an absolute attribute” [18]; or, in other words, that more important to development is
152 the process by which heritable material may manifest different phenotypes than the heritable
153 material itself. However, Waddington’s epigenetic landscape prevailed and the field reinforced
154 a “preinformationist” framework: although the zygote is not a complete miniature version
155 of the mature organism (preformationism), it is indeed a complete blueprint of the mature
156 organism (allowing for some degree of extrinsic influence as described previously and for
157 stochasticity [19, 20]). If this is correct, we must also accept that in the mature human brain there
158 is strictly less—since it is one among many outcomes of the developmental process—non-genetic
159 and non-redundant information than in the human “developmental blueprint” (not surprisingly
160 however, I failed to find a single research paper with such a proposition).

161 This *reductio ad absurdum* shows that the epigenetic landscape framework has forced research
162 to ignore or reject the necessary *emergence* of not only some, but possibly most information
163 content during cell differentiation. Specifically, if additional information content emerges during
164 brain development, what would necessarily preclude information content from emerging in
165 proliferating undifferentiated cells?

166 **A proof-of-principle hypothesis**

167 In the previous two subsections I argued that (i) explaining the self-regulatory dynamics of cell
168 differentiation under the traditional epigenetic landscape approach is a fundamental impossibility,
169 (ii) the constraints regulating the critical variables for cell differentiation must be explicitly
170 uncorrelated to such variables, and (iii) any theory aiming to explain differentiated multicellularity
171 must account for emergent developmental information, which is not structurally but dynamically
172 embodied (that is, dependent on the extracellular context). Consequently, in this work I designed
173 a computational analysis to search for constraints as defined in (ii) because their existence is,
174 ultimately, the proof of principle for the theory referred to in (iii).

175 The specific objects of study were the combinatorial constraints on histone H3 post-translational
176 modifications—also known simply as histone H3 crosstalk—because of their strong statistical
177 relationship with transcriptional levels [21]. Notably, several high-throughput studies have
178 underscored already the relevance of histone crosstalk by identifying highly significant pairwise
179 relationships between post-translational modifications [22, 23, 24, 25].

180 Under these considerations, I defined the working hypothesis as follows: *for any given cell*
181 *differentiation state and within genomic regions adjacent to transcription start sites, the component of*
182 *pairwise histone H3 crosstalk that is explicitly uncorrelated to transcriptional levels associates with*
183 *that differentiation state (Figure 1B, black dashed arrow). Importantly, the null hypothesis (that*
184 *is, no significant relationship exists between cell differentiation states and histone H3 crosstalk*
185 *uncorrelated to mRNA levels) is further supported by the epigenetic landscape approach: if*
186 *changes in mRNA levels not only associate with cell differentiation states [26, 27, 28] but also*
187 *explain them completely, an additional non-epigenetic yet differentiation-associated level of*
188 *constraints on histone H3 crosstalk is unparsimonious or even superfluous.*

189 For the computational analysis I used publicly available tandem datasets of ChIP-seq (chromatin
190 immunoprecipitation followed by high-throughput sequencing) on histone H3 modifications and
191 RNA-seq (transcriptome high-throughput sequencing) on mRNA for *Homo sapiens*, *Mus musculus*,
192 and *Drosophila melanogaster* (see [Materials and Methods](#)). Its basis was to define a numeric
193 profile *ctalk_non_epi*, which represents the strength and sign of pairwise partial correlations
194 between histone H3 modification states controlling for mRNA levels within genomic regions
195 adjacent to RefSeq transcription start sites. In other words, *ctalk_non_epi* profiles represent the
196 non-epigenetic component of pairwise histone H3 crosstalk (see decomposition as a sum of two
197 covariances in [Figure 1B](#)) in genomic regions where the epigenetic component is significant.

198 The hypothesis testing rationale was to apply unsupervised hierarchical clustering on the
199 *ctalk_non_epi* profiles for different cell datasets in all three organisms, using nonparametric
200 bootstrap resampling to assess cluster significance [29]. If the null hypothesis is true, the
201 obtained clusters will be statistically insignificant, or else they will not associate with cell
202 differentiation states.

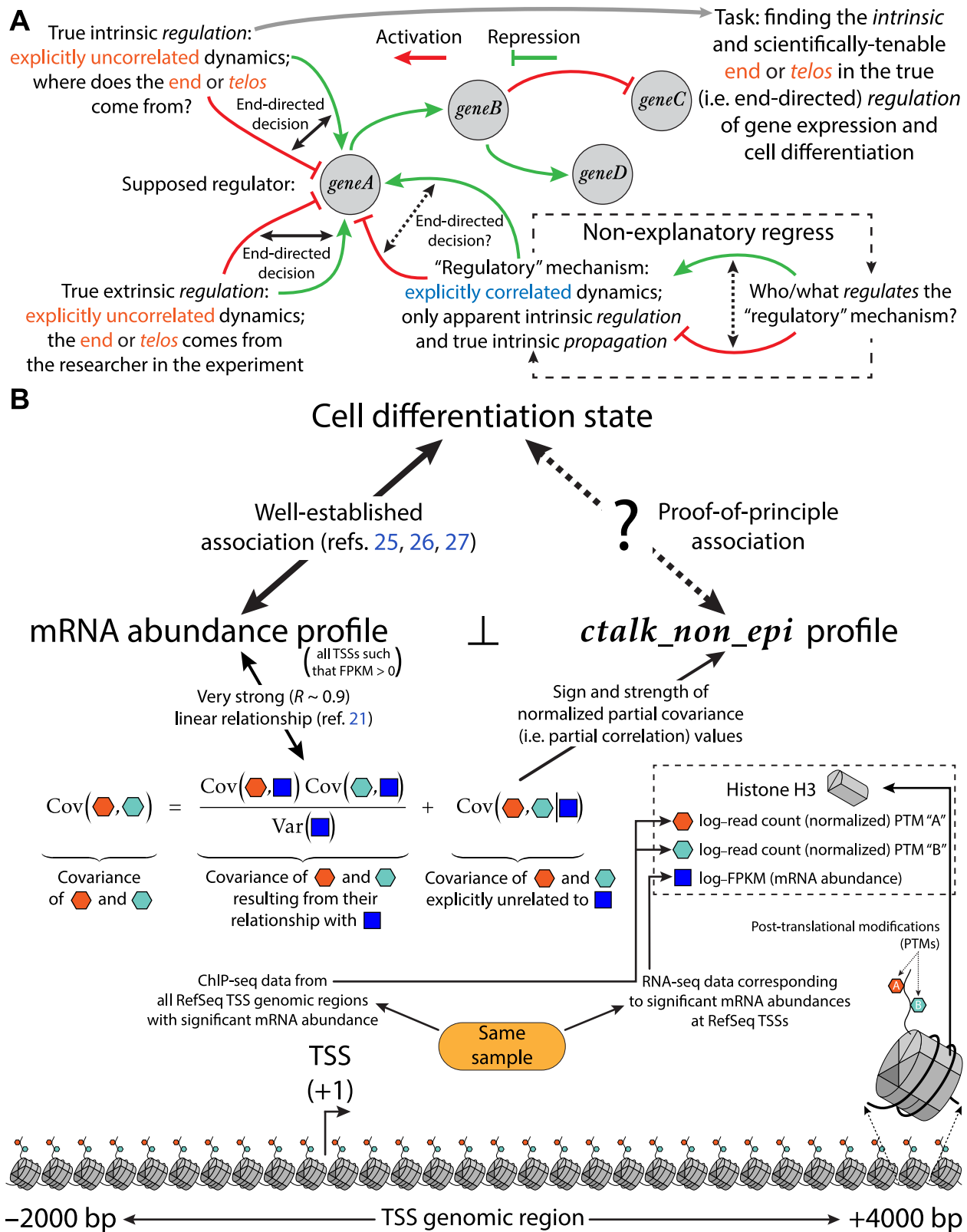


Figure 1: (A) Explanatory limitation of the epigenetic landscape approach in terms of the intrinsic regulation of gene expression. (B) Scheme of the proof-of-principle hypothesis described in the introduction and the computational analysis conducted for its testing (see details in Materials and Methods).

203 Results

204 In all analyses performed, *ctalk_non_epi* profiles fell into statistically significant clusters that
205 associate with cell differentiation states in *Homo sapiens*, *Mus musculus*, and *Drosophila melanogaster*.
206 Moreover, in these results *ctalk_non_epi* profiles associated with cell differentiation states at
207 least as strongly as did mRNA abundance² profiles (as mentioned earlier, the relationship
208 between transcriptional and cell differentiation states is known and well-established [26, 27, 28]).
209 In summary, for all three organisms analyzed, the null hypothesis had to be consistently rejected,
210 indicating that the proof of principle described in the [introduction](#) was obtained.

211 The embryonic stem cells *ctalk_non_epi* profile differs significantly from 212 those of differentiated cell types in *Homo sapiens*

213 Using data for nine different histone H3 modifications (for details see [Materials and Methods](#)),
214 *ctalk_non_epi* profiles were computed for six human cell types. From these, all profiles
215 corresponding to differentiated cell types, namely HSMM (skeletal muscle myoblasts), HUVEC
216 (umbilical vein endothelial cells), NHEK (epidermal keratinocytes), GM12878 (B-lymphoblastoids),
217 and NHLF (lung fibroblasts) fell into the largest statistically significant cluster. Such
218 significance was expressed in the obtained *au* (approximately unbiased) and *bp* (bootstrap
219 probability) significance scores, which were greater or equal than 95 ([Figure 2A, cluster #4](#)).
220 The *ctalk_non_epi* profile identified as dissimilar (i.e. excluded from the largest significant cluster)
221 was the one corresponding to H1-hESC embryonic stem cells.

222 For comparison and positive control, mRNA abundance profiles for the six cell types were
223 constructed from RNA-seq data (the same values that are controlled for in the computation
224 of *ctalk_non_epi* profiles) and then hierarchically clustered. As expected, the transcriptional
225 profile corresponding to H1-hESC (embryonic stem cells) was identified as significantly dissimilar,
226 i.e. resulted excluded from the largest significant cluster ([Figure 2B, cluster #3](#)), although in this
227 case it was excluded along with the GM12878 B-lymphoblastoids profile.

228 The *ctalk_non_epi* profiles associate with cell differentiation states in 229 *Mus musculus*

230 The analysis for mouse comprised five histone H3 modifications in five cell types. As in
231 *Homo sapiens* the *ctalk_non_epi* profiles fell into significant clusters that associate with
232 cell differentiation states. The five comprised cell type datasets were 8-weeks-adult heart,
233 8-weeks-adult liver, plus three datasets of E14 embryonic stem cells after zero, four, and six
234 days of differentiation respectively. All three E14 *ctalk_non_epi* profiles fell into a significant
235 cluster ([Figure 2C, cluster #2](#)) and within it, the profiles corresponding to latter time points
236 (four and six days of differentiation) fell into another significant cluster ([Figure 2C, cluster #1](#)).

²Represented by log₂-transformed FPKM values.

237 Additionally, the liver *ctalk_non_epi* profile was found to be more similar to the profiles of the
238 least differentiated states than the heart profile (**Figure 2C, cluster #3**).

239 Mouse mRNA abundance profiles also fell into significant clusters that associate with cell
240 differentiation states as expected (**Figure 2D, clusters #1, #2 and #3**). As *ctalk_non_epi* profiles
241 did, transcript abundance profiles resolved a significant difference between the earliest time point
242 (zero days of differentiation) and latter time points (**Figure 2D, cluster #1**).

243 **The *ctalk_non_epi* profiles associate with developmental periods and** 244 **time points in *Drosophila melanogaster***

245 In the final analysis, *ctalk_non_epi* profiles were computed from data for six histone H3
246 modifications in nine periods/time points throughout *Drosophila melanogaster* development
247 (0-4h, 4-8h, 8-12h, 12-16h, 16-20h and 20-24h embryos; L1 and L2 larval stages; pupae). As
248 observed in human and mouse profiles, fruit fly *ctalk_non_epi* profiles fell into clusters that
249 also associate strongly with the degree of cell differentiation (derivable from the degree of
250 development). One significant cluster grouped *ctalk_non_epi* profiles of earlier developmental
251 periods (**Figure 2E, cluster #5**) apart from later development profiles. Two more significant
252 clusters grouped later time point *ctalk_non_epi* profiles (**Figure 2E, cluster #3**) and separated
253 the L2 larvae profile (**Figure 2E, cluster #7**) from all other profiles.

254 General *ctalk_non_epi* cluster structure is not entirely consistent with developmental chronology
255 as the pupae profile (**Figure 2E, cluster #7**) shows. It must be noted however that, unlike
256 *Homo sapiens* and *Mus musculus* data where each *ctalk_non_epi* profile represented a specific or
257 almost specific differentiation state, each *Drosophila melanogaster* data set was obtained by the
258 authors from whole specimens (embryos, larvae and pupae). Especially for later development,
259 this implies that each *ctalk_non_epi* profile has to be computed from more than one partially
260 differentiated cell type at the same developmental period, thus limiting to a certain extent the
261 power of the analysis. This caveat in fact highlights the overall *ctalk_non_epi* cluster consistence
262 with developmental chronology, particularly when compared with that obtained from mRNA
263 levels as will be detailed next.

264 The mRNA abundance profiles in *D. melanogaster* yielded a general cluster structure much
265 less consistent with developmental chronology than the obtained from *ctalk_non_epi* profiles.
266 For example, the profile for 0-4h embryos fell into the same significant cluster with the
267 profiles for 16-20h and 20-24h embryos (**Figure 2F, cluster #3**). Additionally, the profile
268 for 12-16h embryos fell into the same significant cluster with the profiles for L1 and
269 L2 larvae (**Figure 2F, cluster #5**).

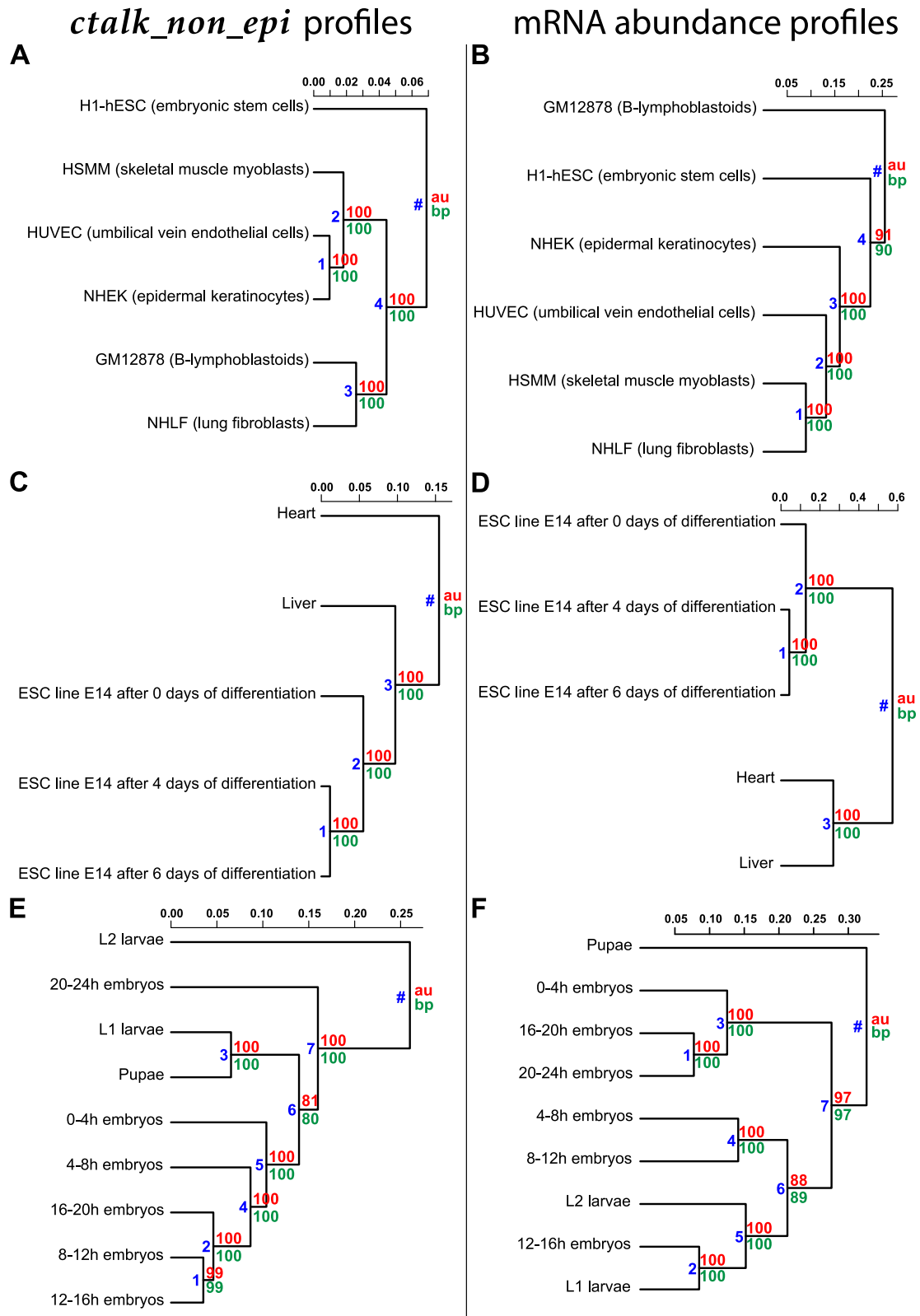


Figure 2: Unsupervised hierarchical clustering of *ctalk_non_epi* profiles and mRNA abundance profiles for *Homo sapiens* (A, B), *Mus musculus* (C, D), and *Drosophila melanogaster* (E, F). Metric: correlation ($1 - r$). Linkage method: “average” (also known as UPGMA). Significance scores [29]: **au** (approximately unbiased) and **bp** (bootstrap probability). Significant clusters were identified as those for which **au** and **bp** ≥ 95 . Cluster numbers are in blue.

270 Discussion

271 Beyond the obtained proof of principle

272 The most important aspect of the previously presented results is not the statistically significant
273 relationship between *ctalk_non_epi* profiles and cell differentiation states but instead the nature
274 of the constraints represented by *ctalk_non_epi* profiles (provided such relationship exists). By
275 definition, *ctalk_non_epi* profiles represent the strength and sign of pairwise partial correlations
276 (with mRNA levels as control variable) computed from observed histone modification states; the
277 same observed states that previous research has shown able to predict mRNA levels with high
278 accuracy ($R \sim 0.9$) [21]. It follows directly from these considerations that, for all three analyzed
279 organisms within regions adjacent to transcription start sites (henceforth TSSs), histone H3
280 modification states are subject to an additional type of constraints that are explicitly uncorrelated
281 to mRNA levels and associated with cell differentiation states. In other words two systems,
282 mutually uncorrelated and yet both associated to cell differentiation states, *simultaneously*
283 constrain histone H3 modification states.

284 Still, any theory of differentiated multicellularity developed on the basis of the critique of the
285 traditional approach presented in the [introduction](#) and on the obtained proof of principle must
286 address these eight fundamental questions:

287
288 **Q1** Since the constraints defining the proof of principle are explicitly uncorrelated to mRNA
289 levels by definition, how do they come to be associated with cell differentiation states?

290 **Q2** If they are indeed necessary for the intrinsic regulation of gene expression during cell
291 differentiation, how is such regulation exerted?

292 **Q3** Can the work exerted by these constraints be regarded as biologically meaningful
293 information? If so, what is the content of this information?

294 **Q4** Can they account for the remarkable and characteristic robustness of cell differentiation
295 with respect to even moderate perturbations?

296 **Q5** How do these constraints relate to the evolution of metazoans? Is this relationship
297 extendable to the evolution of other differentiated multicellular lineages such as plants?

298 **Q6** Are histone H3 modification states ultimately cause or effect of transcriptional states?
299 (This last question is a rehash of a very important point raised previously by Peter Fraser
300 and Wendy Bickmore [30].)

301 **Q7** Why undifferentiated cells start to differentiate in the embryo at certain time point?

302 **Q8** Reciprocally, why do cells stop differentiating? How does this relate to the termination of
303 the ontogenetic process?

304 **Problems with current views on the self-regulation of cell differentiation**
305 **and the evolution of multicellularity**

306 Since Ernst Haeckel’s “gastraea theory” [31], the most plausible models aimed to explain the
307 evolution of differentiated multicellularity are fundamentally divorced from the epigenetic
308 landscape model assumed to explain the self-regulatory dynamics underpinning differentiated
309 multicellularity. This is because Haeckel’s account and the models built upon it rely on the gradual
310 specialization of same-species (or even different-species [32]) cell colonies or aggregations [33, 34,
311 35, 36, 37, 38, 39] while the developmental process starts from a single cell (zygote) or, in other
312 words, “from the inside out”. Since differentiated multicellularity is a single phenomenon whose
313 evolution and self-regulation have been tackled by research under such divergent approaches,
314 the resulting explanatory account is thus insufficiently substantiated as a whole, especially
315 considering its lack of parsimony.

316 Notably, however, some “non-epigenetic” hypotheses have been advanced aiming to explain
317 the dynamics and/or informational requirements of cell-differentiation (which in turn could
318 provide some hints on the evolution of multicellularity). One of them, proposed by
319 Alan Turing in “The Chemical Basis of Morphogenesis” [40], holds that spontaneous intercellular
320 reaction-diffusion patterns are responsible for morphogenesis (and for cell differentiation as a
321 consequence). Whereas Turing’s model has been tested in terms of chemical differentiation of
322 synthetic (non-living) “cells” [41] it does not explain, among other things, the critical relationship
323 between real differentiating/differentiated cells in terms of their function and dependence with
324 respect to the individuated multicellular organism as a whole. Another relevant hypothesis is
325 “darwinian cell differentiation” proposed by J. J. Kupiec, according to which gene expression
326 instability and stochasticity, in the context of external metabolic substrate gradients, creates
327 an intrinsic natural-selection-like mechanism able to drive the differentiation process [42].
328 A third “non-epigenetic” hypothesis, advanced by Andras Paldi, is that cell fate decisions
329 are the result of the characteristic coupling of gene expression and metabolism: fates are
330 determined by fluctuations in the nutrient/oxygen ratio, which are driven by the necessity to
331 maintain the dissipative nature of the metabolic network, which in turn must be redox-neutral
332 at all times [43].

333 At large, to my knowledge all explanatory accounts of the evolution and/or self-regulation
334 of differentiated multicellularity suffer a combination of some or all the following problems:
335 (i) failure to explain how traits or dynamics that supposedly account for the transition
336 to multicellularity or to cell differentiation have fundamentally analogous counterparts in
337 undifferentiated multicellular or unicellular eukaryotic lineages, (ii) failure to account, at least
338 in principle, for the information required by developmental decisions or in the transition
339 between strictly single-cell-related content to additional multicellular-individual-related content,
340 (iii) failure to explain the reproducible and robust self-regulatory dynamics—apart from
341 the propagatory—of gene expression during cell differentiation, (iv) failure to describe
342 fundamentally and unambiguously the transition between a highly complex or symbiotic
343 cell population/aggregation and a differentiated multicellular organism, (v) lack of parsimony
344 when encompassing both the evolution and self-regulation of differentiated multicellularity as
345 discussed previously, and (vi) unfalsifiability.

346 In terms of overcoming these problems, it must be noted that Turing’s and Kupiec’s hypotheses
347 encompassed a variable that, I submit, is critical to the solution of the riddle: certain gradients
348 emerging in the extracellular space—not yet identified, but both fundamentally conceivable and
349 experimentally verifiable—can elicit changes in histone modifications explicitly uncorrelated to
350 gene expression profiles. It is possible that Kupiec in particular did not consider this possibility
351 because his attempt to explain cell differentiation relied only on random variation and selection,
352 ruling out with this any explanatory role of emergent systems and properties.

353 In contrast to current hypotheses, the falsifiable theory to be proposed here regards the
354 multicellular organism as a higher-order system that *emerges* from proliferating undifferentiated
355 cells and *then* is subject to natural selection (as emerged the very first self-replicating and
356 self-repairing system—ancestor of all known living organisms—beyond any reasonable doubt).
357 Importantly, the theoretical development in this work is not based on the substrate-based³ concept
358 of irreducible emergence (fundamentally refuted by Jaegwon Kim [44, 45]) but instead converged
359 (from the strict *explicitly-uncorrelated-constraint-dynamics* condition argued in the [introduction](#))
360 into what can be described as the constraint-based⁴ concept of emergence for higher-order
361 teleological systems, pioneered in a broader perspective by Terrence Deacon in 2011 [46].
362 Importantly, this formulation of emergence does not build upon the traditional concepts of *telos*
363 or “final cause”—logically inconsistent and/or non-explanatory—but instead redefines the *telos*
364 as a thermodynamically spontaneous, intrinsic constraint whose causal power is exerted at the
365 present instant.

³Understood as molecules and their realizable interactions, which define the state space in a dynamical systems model such as the epigenetic landscape.

⁴Understood as the dynamics explicitly *excluded* from realization in the system.

366 Preliminary theoretical definitions and notation

367 Before enunciating the theory, I must introduce the following new definitions and notation
368 regarding molecular dynamics and spatial topology:

369 **Context** $X_{(i;t)}$ is the i^{th} cell of a given organism or cell population of the eukaryotic
370 species X at a given instant t . In the same logic, *the following concepts must be*
371 *understood in instantaneous terms.*

372 $S_E(X_{(1;t)}, \dots, X_{(n;t)})$ **Extracellular space:** The entire space in an organism or cell population that
373 is not occupied by its n cells themselves at a given instant t . Positions in
374 $S_E(t)$ will be specified in spherical coordinates, namely r (radial distance), θ
375 (azimuthal angle), and ϕ (polar angle).

376 $C_W(X_{(i;t)})$ **Waddington's constraints:** The constraints associating certain subsets of the
377 spatially-specified molecular nuclear phenotype of $X_{(i;t)}$ with the instantaneous
378 transcription rates at the transcription start sites (TSSs), provided changes
379 in these Waddington's constraints $C_W(X_{(i;t)})$ are *explicitly uncorrelated* with
380 changes in the genomic sequence.

381 $F_W(X_{(i;t)})$ **Waddington's embodiens:** The largest subset of the spatially-specified
382 molecular nuclear phenotype of $X_{(i;t)}$ for which the Waddington's constraints
383 $C_W(X_{(i;t)})$ are significant (e.g. histone H3 post-translational modifications in
384 the TSS-adjacent genomic regions).

385 $C_N(X_{(i;t)})$ **Nanney's constraints:** The constraints associating certain subsets of the
386 spatially-specified molecular nuclear phenotype of $X_{(i;t)}$ with the Waddington's
387 embodiens $F_W(X_{(i;t)})$, provided changes in these Nanney's constraints
388 $C_N(X_{(i;t)})$ are *explicitly uncorrelated* with changes in the instantaneous
389 transcription rates at the TSSs. In this work Nanney's constraints were
390 represented by the *ctalk_non_epi* profiles.

391 $F_N(X_{(i;t)})$ **Nanney's embodiens:** The largest subset of the spatially-specified molecular
392 nuclear phenotype of $X_{(i;t)}$ for which the Nanney's constraints $C_N(X_{(i;t)})$
393 are significant. Crucially, histone H3 post-translational modifications in the
394 TSS-adjacent regions—as inferable from the [Results](#)—can be specifiable as
395 Waddington's embodiens F_W and as Nanney's embodiens F_N *simultaneously*.

396 $F_N^{\rightarrow}(X_{(i;t)})$ **Nanney's extracellular propagators:** The subset of the entire
397 spatially-specified molecular phenotype of $X_{(i;t)}$ that excludes Nanney's
398 embodiens $F_N(X_{(i;t)})$ but is (i) secreted into the the extracellular space S_E and
399 (ii) capable of eliciting a change (via facilitated diffusion/signal transduction) in
400 Nanney's embodiens F_N within other cells after a certain time interval Δt .

401 **A general theory of differentiated multicellularity**

402 This theory mainly aims to explain how cell differentiation emerges in the ontogeny of extant
403 multicellular lineages and how differentiated multicellular lineages emerged throughout evolution.
404 To highlight the similarities of both phenomena at the most fundamental level, the theory will be
405 proposed in parts described in parallel. Each part will be described in terms of the evolution
406 of an ancestor eukaryotic species U towards differentiated multicellularity and in terms of
407 the ontogenetic process starting from the zygote of a differentiated multicellular species D .
408 Importantly, and although its proof of principle was obtained from high-throughput metazoan
409 data, this theoretical description makes no assumption whatsoever about a specific multicellular
410 lineage. This is why it is referred to as a general theory here and also in the title.

411

412 **Part I The unicellular (or undifferentiated multicellular) ancestor** 413 **(Evolution)**

- 413 • $U_{(i;t_{U_0})}$ is the i^{th} cell in a population of the unicellular (or undifferentiated
414 multicellular) species U (**Figure 3A, top**).
- 415 • $U_{(i;t_{U_0})}$ displays Waddington's embodiars $F_W(U_{(i;t_{U_0})})$ (e.g. histone
416 post-translational modifications able to elicit changes in transcriptional
417 rates) but cell differentiation is not possible.
- 418 • Certain constraints exist on Waddington's embodiars $F_W(U_{(i;t_{U_0})})$ that are
419 *explicitly uncorrelated* with transcriptional rates. In other words, significant
420 Nanney's constraints $C_N(U_{(i;t_{U_0})})$ exist.
- 421 • However, the propagation (if any) of Nanney's constraints C_N is confined
422 to $U_{(i;t_{U_0})}$. In other words, Nanney's extracellular propagators F_N^{\rightarrow} do not
423 exist in $U_{(i;t_{U_0})}$.

424 **Part I The differentiated multicellular organism's zygote** 425 **(Ontogeny)**

- 425 • $D_{(1;t_{D_0})}$ is a zygote of the extant differentiated multicellular
426 species D (**Figure 3A, bottom**).
- 427 • Like $U_{(i;t_{D_0})}$, $D_{(1;t_{D_0})}$ displays displays Waddington's embodiars
428 $F_W(D_{(1;t_{D_0})})$ (e.g. histone post-translational modifications able to elicit
429 changes in transcriptional rates) but cell differentiation is not observed *yet*.
- 430 • Certain constraints exist on Waddington's embodiars $F_W(D_{(1;t_{D_0})})$ that are
431 *explicitly uncorrelated* with transcriptional rates. In other words, significant
432 Nanney's constraints $C_N(D_{(1;t_{D_0})})$ exist.
- 433 • Unlike in $U_{(i;t_{D_0})}$, the propagation of Nanney's constraints C_N is *not*
434 confined to $D_{(1;t_{D_0})}$. In other words, Nanney's extracellular propagators F_N^{\rightarrow}
435 do exist in $D_{(1;t_{D_0})}$.

436 **Part II**
437 **(Evolution)**

The necessary novel alleles

- 438 • At some time point $(t_M - \Delta t_M) > t_{U_0}$ during evolution the genome of
439 certain $U_{(k;t_M-\Delta t_M)}$ cell suffers a change (**Figure 3A to 3B**) such that
440 it now synthesizes a molecule specifiable as a Nanney's extracellular
441 propagator F_N^{\rightarrow} .
- 442 • As described in the preliminary definitions, this means a molecular
443 substrate is synthesized that is membrane exchangeable and, once
444 entering the cell, is also able to elicit a change in Nanney's
445 embodiars $F_N(U_{(i;t_{U_0})})$ (e.g. histone post-translational modifications).
446 Importantly, this change is *explicitly uncorrelated* with the transcriptional
447 rates at the instant it is elicited.
- 448 • The genetic change implies that the genome now codes for all gene products
449 necessary for the synthesis, facilitated diffusion/signal transduction of the
450 novel Nanney's extracellular propagator(s) F_N^{\rightarrow} .
- 451 • Importantly, the novel alleles are a necessary but not sufficient condition
452 for differentiated multicellularity (**Figure 3B**).

453 **Part II**
454 **(Ontogeny)**

The already present necessary alleles

- 455 • At any instant $(t_D - \Delta t_D) > t_{D_0}$ the genome of any cell $D_{(i;t_D-\Delta t_D)}$
456 in the zygote's offspring is similar to the genome of the cell
457 $U_{(k;t_M-\Delta t_M)}$ (see **Figure 3B, top**) in the sense that both genomes code
458 for Nanney's extracellular propagators F_N^{\rightarrow} .
- 459 • Importantly, the alleles specified in genome of the zygote $D_{(1;t_{D_0})}$ —and in
460 the genome of any cell in its offspring—are a necessary but not sufficient
461 condition for cell differentiation (**Figure 3B**).

463 **Part III**
464 **(Evolution &**
465 **Ontogeny)**

Diffusion flux of Nanney's extracellular propagators and the geometry of
466 **the extracellular space S_E**

- 467 • The existence of Nanney's extracellular propagators F_N^{\rightarrow} allows to define a
468 scalar field⁵ Φ_N describing the concentration of F_N^{\rightarrow} in the extracellular
469 space S_E at any instant t .
- 470 • When the number of cells is small enough, diffusion flux is fast enough to
overtake the spatial constraints imposed by the relatively simple geometry
of S_E .

⁵A scalar field is a function associating a scalar (here concentration of Nanney's extracellular propagators F_N^{\rightarrow}) to every point in space.

- 471 • Therefore, under these conditions the associated gradient⁶ $\vec{\nabla} \Phi_N$ remains
 472 in magnitude—anywhere in S_E —under a certain critical value V_M for the
 473 offspring of the cell $U_{(k;t_M-\Delta t_M)}$ and under a critical value V_D for the
 474 offspring of the zygote $D_{(1;t_{D_0})}$ (**Figure 3B, bottom**).
- 475 • Importantly, the constraints represented by the gradient $\vec{\nabla} \Phi_N$ imply there
 476 is free energy available—whether or not there is cell differentiation—which,
 477 as will be described later, is in fact partially utilized as work in the
 478 emergence of new information content.
- 479
- 480

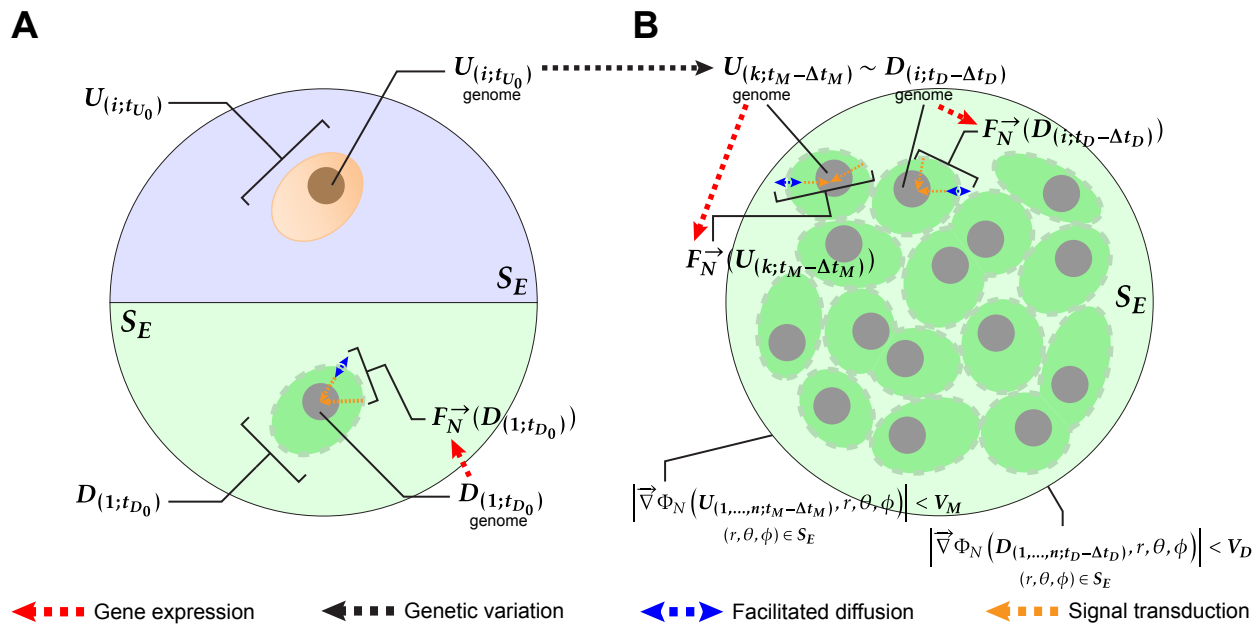


Figure 3: A, (top): A cell of the unicellular and undifferentiated ancestor species U . **A (bottom):** A zygote of the multicellular species D . **A (top) to B (top):** The necessary genetic change for differentiated multicellularity occurs in the species U . **B (top):** The similar and necessary alleles are now present in both species. **B (bottom):** Cells proliferate but no significant $\vec{\nabla} \Phi_N$ gradients form yet in S_E and no differentiation is observed.

⁶The gradient vector field $\vec{\nabla}$ of a scalar function (in this context, the scalar field Φ_N) is a vector operation that generalizes the concept of derivative represented by the differential operator—denoted by the ∇ (nabla) symbol and also called “del”—to more than one dimension.

481 **Part IV**
482 **(Evolution)**

The emergent transition to differentiated multicellularity

- 483 • At some later but relatively close instant t_M , cell proliferation yields a
484 significantly larger population. Now diffusion flux of Nanney's extracellular
485 propagators F_N^{\rightarrow} is no longer able to overtake the increasing spatial
486 constraints in the extracellular space S_E .
- 487 • Under these conditions a significant gradient, in magnitude equal
488 or greater—anywhere in S_E —than the critical value V_M forms,
489 i.e. $\left| \vec{\nabla} \Phi_N(U_{(1;t_M)}, \dots, U_{(n;t_M)}, r, \theta, \phi) \right| \geq V_M, (r, \theta, \phi) \in S_E$ (**Figure 4,**
bottom-left).
- 490 • As consequence, Nanney's extracellular propagators F_N^{\rightarrow} diffuse
491 differentially into each cell, yielding unprecedented differential Nanney's
492 constraints $\{C_N(U_{(1;t_M)}), \dots, C_N(U_{(n;t_M)})\}$ in the cells' nuclei by virtue of
493 no cell or gene product in particular but, importantly, of the constraints
494 imposed by the entire proliferating cell population on the diffusion flux of
495 F_N^{\rightarrow} in S_E .
- 496 • These differential Nanney's constraints C_N in turn elicit differential changes
497 in Waddington's embodiery $\{F_W(U_{(1;t_M)}), \dots, F_W(U_{(n;t_M)})\}$ within the cells'
498 nuclei (**Figure 4, top-left**), thus they now constrain the instantaneous
499 transcription rates in a differential and explicitly uncorrelated manner.
500 This is how multicellular lineages, displaying self-regulated changes in gene
501 expression during ontogeny, evolved.

503 **Part IV**
504 **(Ontogeny)**

The emergent transition to cell differentiation

- 505 • At some later but relatively close instant t_D , embryonic growth yields
506 certain number of undifferentiated cells. Now diffusion flux of Nanney's
507 extracellular propagators is no longer able to overtake the increasing spatial
508 constraints in the extracellular space S_E .
- 509 • Under these conditions a significant gradient, in magnitude equal
510 or greater—anywhere in S_E —than the critical value V_D forms,
511 i.e. $\left| \vec{\nabla} \Phi_N(D_{(1;t_D)}, \dots, D_{(n;t_D)}, r, \theta, \phi) \right| \geq V_D, (r, \theta, \phi) \in S_E$ (**Figure 4,**
bottom-right, see also question Q7).
- 512 • As consequence, Nanney's extracellular propagators F_N^{\rightarrow} diffuse
513 differentially into each cell, yielding unprecedented differential Nanney's
514 constraints $\{C_N(D_{(1;t_D)}), \dots, C_N(D_{(n;t_D)})\}$ in the cells' nuclei by virtue of
515 no cell or gene product but, importantly, of the constraints imposed by
516 the entire growing embryo on the diffusion flux of Nanney's extracellular
517 propagators in the extracellular space S_E .

518
519
520
521
522
523
524
525

- These differential Nanney's constraints C_N in turn elicit differential changes in Waddington's embodiars $\{F_W(D_{(1;t_D)}), \dots, F_W(D_{(n;t_D)})\}$ within the cells' nuclei (**Figure 4, top-right**), thus they now constrain the instantaneous transcription rates in a differential and explicitly uncorrelated manner. This is how undifferentiated cells start to differentiate, displaying self-regulated changes in gene expression during ontogeny (see question Q1).

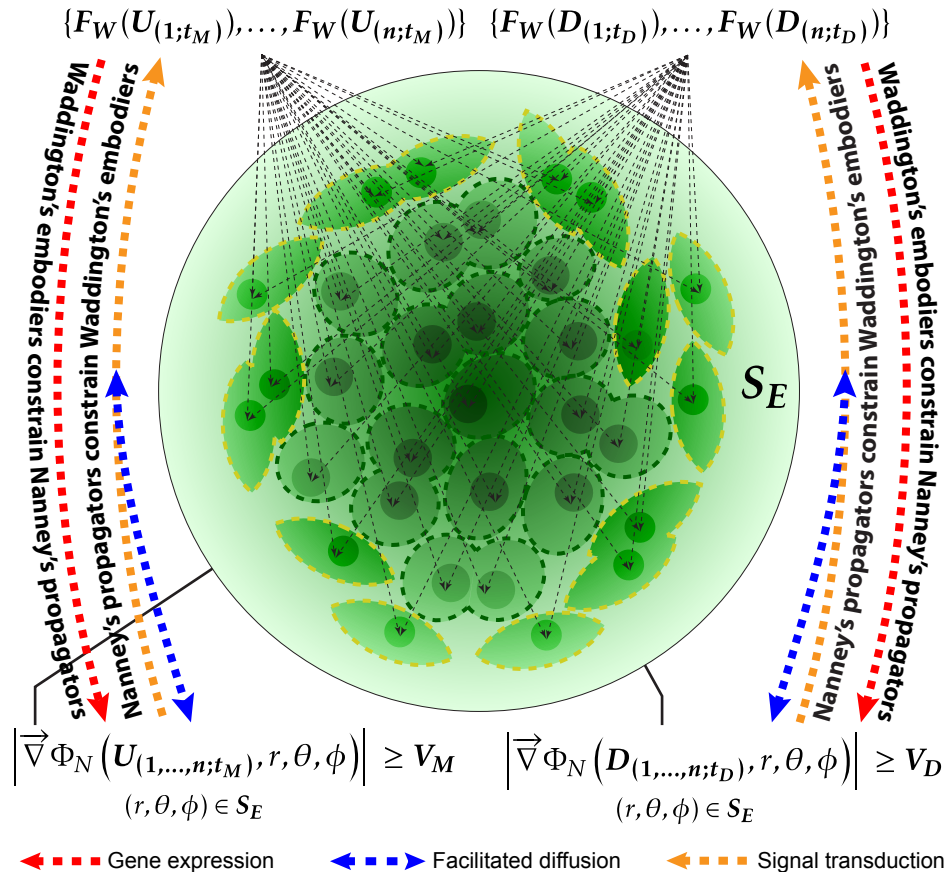


Figure 4: The emergent transition to differentiated multicellularity/cell differentiation. **Dashed arrows:** The intrinsic higher-order constraint emerges when significant gradients $\vec{\nabla} \Phi_N$ (bottom) couple the lower-order Nanne's constraints C_N and Waddington's constraints C_W synergistically across S_E . **Top:** Waddington's embodiars F_W constrain—via gene expression (red dashed arrows)—the membrane exchange of Nanne's extracellular propagators F_N^{\rightarrow} driven by the gradients. **Bottom:** The gradients $\vec{\nabla} \Phi_N$ constrain in turn—via facilitated diffusion/signal transduction of F_N^{\rightarrow} (blue and orange dashed arrows)—Waddington's embodiars F_W and as a consequence constrain also transcription rates and gene expression levels.

526 **Part V**
527 **(Evolution)**

What was the evolutionary breakthrough?

- 528 • Since the oldest undisputed differentiated multicellular organisms appear in
529 the fossil record around 2.8 billion years after the first stromatolites [47], the
530 necessary genetic change from the genome of the cell $U_{(i;t_{U_0})}$ to the genome
531 of the cell $U_{(k;t_M-\Delta t_M)}$ can be safely regarded as a highly improbable step.
- 532 • Nevertheless, the major evolutionary breakthrough was not genetic but
533 instead the unprecedented dynamical regime emerging from proliferating
534 eukaryote cells at t_M , or in more general terms at $\{t_{M_1}, \dots, t_{M_n}\}$ throughout
535 evolution since extant differentiated multicellular organisms constitute a
536 paraphyletic group [48, 35].
- 537 • This novel dynamical regime emerges as a higher-order constraint⁷ from the
538 synergistic coupling of the lower-order Waddington's constraints C_W and
539 Nanney's constraints C_N , able now to propagate through the extracellular
540 space S_E (Figure 4, dashed arrows).
- 541 • Although dependent on the novel alleles in the genome of $U_{(k;t_M-\Delta t_M)}$
542 to emerge given enough cell proliferation, this system is not a network
543 of epigenetic mechanisms—however complex—but instead a particular
544 instantiation of a *teleodynamic system*, proposed by Terrence Deacon in his
545 *theory of biological individuality by constraint coupling and preservation*⁸ [46],
546 which is presented to and shaped by natural selection at each instant. In
547 this context, environmental constraints as oxygen availability [49] and even
548 gravity (see Corollary #5) filter out specific emergent multicellular dynamics
549 that are incompatible with them.
- 550 • In summary, the critical evolutionary novelty was the unprecedented
551 multicellular individual or multicellular *self*, which can be described as an
552 intrinsic, higher-order dynamical constraint that emerges spontaneously
553 from a particular class of proliferating eukaryotic cells. Being a higher-order
554 *constraint*, this multicellular *self* is causally-efficacious when regulating its
555 intrinsic dynamics or its surroundings.

556 **Part V**
557 **(Ontogeny)**

Who is regulating cell differentiation?

- 558 • Contrary to what could be derived from Turing's approach [40], the theory
559 hereby proposed does *not* regard the significant proliferation-generated
560 extracellular gradient, i.e. $|\vec{\nabla} \Phi_N| \geq V_D$ (anywhere in S_E), as the
fundamental regulator of the cell differentiation process.

⁷Understood as the states explicitly excluded from being realized in the dynamics of the system.

⁸Although Deacon himself named his theory *emergent dynamics*, I am proposing here this longer but more descriptive name.

- 561
- 562
- 563
- 564
- 565
- 566
- 567
- 568
- 569
- 570
- 571
- Whereas differential Nanney’s constraints $\{C_N(D_{(1;t_D)}), \dots, C_N(D_{(n;t_D)})\}$ are *regulatory constraints* with respect to Waddington’s embodi-ers $\{F_W(D_{(1;t_D)}), \dots, F_W(D_{(n;t_D)})\}$ as described in Part IV-Ontogeny (see Figure 4, blue/orange dashed arrows), the reciprocal proposition is also true. Namely, Waddington’s constraints $\{C_W(D_{(1;t_D)}), \dots, C_W(D_{(n;t_D)})\}$ are *explicitly uncorrelated* to Nanney’s constraints, thus they are in turn *regulatory constraints* with respect to Nanney’s extracellular propagators $\{F_N^{\rightarrow}(D_{(1;t_D)}), \dots, F_N^{\rightarrow}(D_{(n;t_D)})\}$, e.g. changes in the expression of the protein channels, carriers or membrane receptors necessary for the facilitated diffusion/signal transduction of Nanney’s extracellular propagators (see Figure 4, red dashed arrows).
 - Consequently, only if the explicitly uncorrelated Waddington’s constraints C_W and Nanney’s constraints C_N ⁹ become synergistically coupled (Figure 4, dashed arrows) across the extracellular space S_E true intrinsic regulation on the cell differentiation process is possible.
 - This implies in turn that both chromatin states and transcriptional states are simultaneously cause and effect with respect to each other (this regime, intuitively describable as “chicken-egg” dynamics, is the answer this theory provides to question Q6).
 - The true regulator of the cell differentiation process is then the developing multicellular organism itself. This is because the multicellular organism *is* the causally-efficacious, higher-order constraint emerging from and regulating *ipso facto* Nanney’s constraints C_N and Waddington’s constraints C_W (when coupled synergistically across the extracellular space S_E) in what would be otherwise a population or colony—however symbiotic—of unicellular eukaryotes (see question Q2).
- 576
- 577
- 578
- 579
- 580
- 581
- 582
- 583
- 584
- 585
- 586
- 587
- 588

589 Part VI Unprecedented multicellular dynamics

590 (Evolution)

- 591
- 592
- 593
- 594
- 595
- Once the necessary alleles for differentiated multicellularity were present in some eukaryotic lineages, phenomena like mutation, gene duplication or alternative splicing—in the loci involved in the synthesis, facilitated diffusion or signal transduction of Nanney’s extracellular propagators F_N^{\rightarrow} —made possible the emergence of a plethora of novel multicellular (*teleodynamic*) regimes.
 - Moreover, the dependence of differentiated multicellularity on one or more coexisting $\vec{\nabla} \Phi_N$ gradients (i.e. constraints on diffusion flux) in S_E , which importantly depend on no cell in particular but on the entire cell population or embryo, yields an important implication in evolutionary terms. That is, since a higher-order constraint is taking over the regulation of changes
- 596
- 597
- 598
- 599
- 600

⁹Both emerge in turn from genetic (i.e. structurally embodied) constraints.

601 in gene expression within individual cells, it is predictable that said cells
602 lose some cell-intrinsic systems that were critical in a time when eukaryotic
603 life was only unicellular, even when compared with their prokaryotic
604 counterparts¹⁰.

605 • In this context a result obtained over a decade ago acquires relevance: in
606 a genome-wide study it was found that that the number of transcription
607 factor genes increases as a power law of the total number of protein coding
608 genes, with an exponent greater than 1. In other words, the need for
609 transcription-factor genetic information increases faster than the total
610 amount of genetic information it is involved in regulating [50]. Remarkably,
611 the eukaryotes analyzed—~10 genomes, most from differentiated
612 multicellular organisms—was the group with the smallest (i.e. closest
613 to linearity) power-law exponent. This means that the most complex
614 organisms require proportionally *less* transcription-factor information. With
615 data available today [51], a reproduction of the aforementioned analysis
616 allowed in this work a robust confirmation: the power-law exponent for
617 unicellular or undifferentiated multicellular eukaryotes is 1.33 ± 0.31
618 (37 genomes), and for differentiated multicellular eukaryotes is 1.11 ± 0.18
619 (67 genomes)¹¹. The previously described loss of lower-order, cell-intrinsic
620 regulatory systems in differentiated multicellular organisms—accounted for
621 by the emergence of higher-order information content (see [Part IX](#))—is
622 entirely consistent with the otherwise counterintuitive differences in
623 power-law exponents.

625 **Part VI** **What does ontogeny recapitulate?** 626 **(Ontogeny)**

- 627 • This theory holds the hereby proposed emergent transition, spontaneous
628 from cell proliferation shortly after Nanney's extracellular propagators F_N^{\rightarrow}
629 appeared, as key to the evolution of any multicellular lineage displaying
630 self-regulated changes in gene expression during cell differentiation.
- 631 • Therefore, this theoretical description rejects the hypothesis that
632 metazoans—or, in general, any multicellular lineage displaying
633 self-regulated cell differentiation—evolved from gradual specialization of
634 single-cell colonies or aggregations [31, 33, 34, 35, 36, 37, 38, 39].
- 635 • Importantly however, this is not to say that potentially precedent traits
636 (e.g. cell-cell adhesion) were necessarily unimportant for the later fitness of
637 differentiated multicellular organisms.

¹⁰T. Deacon generically described this as the offloading of teleodynamic constraints in lower-order systems—at the cost of losing teleodynamic properties—into the higher-order teleodynamic system emerging from them.

¹¹The difference between the two estimates is statistically significant (assessed by 95%-confidence, nonparametric BCa bootstrapping).

- Neither is this to reject Haeckel's famous assertion completely: in every extant multicellular lineage this self-sufficient, self-repairing, self-replicating, and self-regulating system has emerged over and over again from undifferentiated cells and presented itself to natural selection ever since its evolutionary debut. Therefore, at least in this single yet most fundamental sense, ontogeny does recapitulate phylogeny.

Part VII (Evolution & Ontogeny)

The role of epigenetic changes

- Contrary to what the epigenetic landscape framework entails, under this theory the heritable changes in gene expression do not define let alone explain the intrinsic regulation of cell differentiation.
- The robustness, heritability, and number of cell divisions which any epigenetic change comprises are instead adaptations of the higher-order dynamical constraint emergent from individual cells (i.e. the multicellular organism).
- These adaptations have been shaped by natural selection after the emergence of each extant multicellular lineage and are in turn reproduced or replaced by novel adaptations in every successful ontogenetic process.

Part VIII (Evolution & Ontogeny)

Novel cell types, tissues and organs evolve and develop

- Further genetic variation in the novel alleles in the genome of the cell $U_{(k;t_M-\Delta t_M)}$ or the already present alleles in the genome of the $D_{(1;t_{D_0})}$ (e.g. mutation, gene duplication, alternative splicing) imply than one or more than one $\{\vec{\nabla}\Phi_{N_1}, \dots, \vec{\nabla}\Phi_{N_k}\}$ gradients emerge in S_E with cell proliferation.
- A cell type T_j will develop then in a region S_{E_i} of the extracellular space S_E when a relative uniformity of Nanney's extracellular propagators is reached, i.e. $\left(\left|\vec{\nabla}\Phi_{N_1;T_j}\right|, \dots, \left|\vec{\nabla}\Phi_{N_k;T_j}\right|\right) < \left(V_{N_1;T_j}, \dots, V_{N_k;T_j}\right), (r, \theta, \phi) \in S_{E_i}$, where $\left(V_{N_1;T_j}, \dots, V_{N_k;T_j}\right)$ are certain critical values (see a two-cell-type and two-gradient depiction in [Figure 5](#)).
- As highlighted earlier, cell differentiation is not *regulated* by these gradients themselves but by the higher-order constraint emergent from the synergistic coupling of Waddington's constraints C_W and Nanney's constraints C_N across S_E .
- This constraint synergy can be exemplified as follows: gradients $\{\vec{\nabla}\Phi_{N_1}, \dots, \vec{\nabla}\Phi_{N_k}\}$ can elicit changes in gene expression in a number of cells, which in turn may promote the dissipation of the gradients

675
676
677
678
679
680
681
682
683
684
685
686
687
688
689
690
691
692
693
694
695
696
697
698

(e.g. by generating a surrounding membrane that reduces dramatically the effective S_E size) or may limit further propagation of those gradients from S_E into the cells (e.g. by repressing the expression of genes involved in the facilitated diffusion/signal transduction of F_N^{\rightarrow} in S_E).

- Thus, under this theory cell types, tissues, and organs evolved sequentially as “blobs” of relative F_N^{\rightarrow} uniformity in regions $\{S_{E_1}, \dots, S_{E_n}\}$ (i.e. regions of relatively small $\vec{\nabla}\Phi_N$ magnitude) within S_E displaying no particular shape or function—apart from not being incompatible with the multicellular organism’s survival and reproduction—by virtue of genetic variation (involved in the embodiment and propagation of Nanney’s constraints C_N) followed by cell proliferation.
- The F_N^{\rightarrow} -uniformity “blobs” emerged with no function in particular—apart from not being incompatible with the multicellular organism’s survival and reproduction—by virtue of random genetic variation (involved in the embodiment and propagation of Nanney’s constraints C_N) followed by cell proliferation.
- Then, these F_N^{\rightarrow} -uniformity “blobs” were shaped by natural selection from their initially random physiological and structural properties to specialized cell types, tissues, and organs (importantly, such specialization evolves with respect to the emergent intrinsic higher-order constraint proposed here as the multicellular organism). The result of this emergence-selection process is observable in the dynamics characterizing the ontogeny of extant multicellular species (**Figure 6A**).

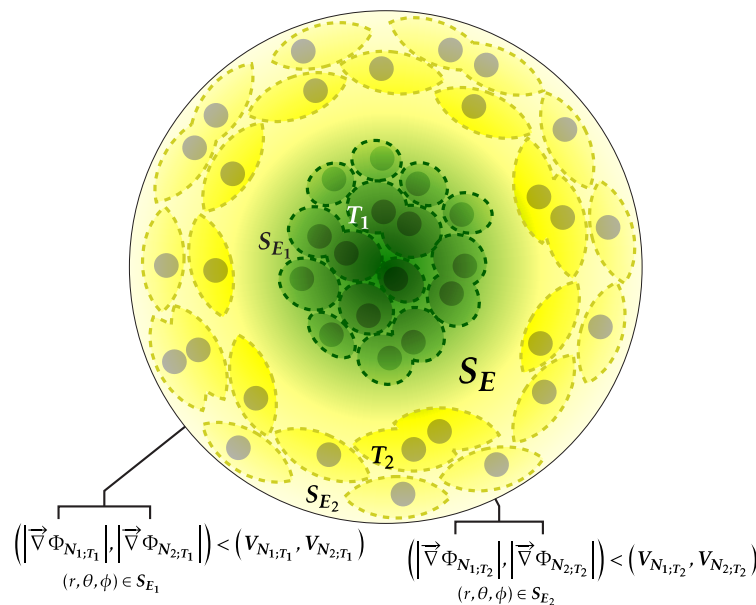


Figure 5: Two distinct cell types T_1 and T_2 develop respectively in regions S_{E_1} and S_{E_2} within S_E characterized by a relative small $\vec{\nabla}\Phi_N$ gradient magnitude, i.e. in extracellular regions of relative F_N^{\rightarrow} uniformity.

699 **Part IX**
700 **(Evolution &**
701 **Ontogeny)**

Emergent *hologenic* information and multicellular self-repair

- 702 • As argued in the [introduction](#), a significant amount of information content
703 has to *emerge* to account for robust and reproducible cell fate decisions and
704 for the self-regulated dynamics of cell differentiation in general.
- 705 • Under this theory, this content emerges when the significant gradient
706 or gradients $\{\vec{\nabla}\Phi_{N_1}, \dots, \vec{\nabla}\Phi_{N_k}\}$ form at some point from proliferating
707 undifferentiated cells, entangling synergistically Nanney’s constraints C_N
708 and Waddington’s constraints C_W across S_E .
- 709 • Crucially, this information is *not* about any coding sequence and
710 its relationship with cell-intrinsic and cell-environment dynamics (i.e.
711 genetic information) *nor* about any heritable gene expression level/profile
712 and its relationship with cell-intrinsic and cell-environment dynamics
713 (i.e. epigenetic information).
- 714 • Instead, this information is *about the multicellular organism as a whole*
715 (understood as the emergent higher-order intrinsic constraint described
716 previously) and also about the environmental constraints under which
717 this multicellular organism develops. For this reason I propose to call this
718 emergent information *hologenic*¹² (see question [Q3](#)).
- 719 • No less importantly, at each instant the multicellular organism is not only
720 interpreting hologenic information—by constraining its development into
721 specific trajectories since it emerges—but also actively generating novel
722 hologenic information (in other words displaying “chicken-egg” dynamics,
723 similar to those described in [Part V-Ontogeny](#)).
- 724 • In the multicellular organism, the subset of the molecular phenotype
725 that conveys hologenic information is not only the subset involved in
726 the gradients $\{\vec{\nabla}\Phi_{N_1}, \dots, \vec{\nabla}\Phi_{N_k}\}$ but the entire subset embodying or
727 propagating Nanney’s constraints C_N .
- 728 • Additionally, since the gradients $\{\vec{\nabla}\Phi_{N_1}, \dots, \vec{\nabla}\Phi_{N_k}\}$ conveying hologenic
729 information depend on no cell in particular—not even on a sufficiently
730 small group of cells—but on the spatial constraints imposed by the entire
731 cell population or embryo, cell differentiation will be robust with respect to
732 moderate perturbations such as some cell loss (see question [Q4](#)).

¹²ὅλος is the ancient Greek for “whole” or “entire”.

731 **Part X**
732 **(Ontogeny)**

Ontogeny ends and cell differentiation “terminates”

- 733 • If under this theory cell differentiation emerges with the proliferation of
734 (at the beginning, undifferentiated) cells, why should it terminate for any
735 differentiation lineage? What is this “termination” in fundamental terms?
- 736 • These are no trivial questions. As an answer to the first, zero net
737 proliferation begs the fundamental question. To the second, a “fully
738 differentiated” cell state condition fails to explain the existence of adult
739 stem cells. To address these issues three considerations are most important:
- 740 (i) For any cell or group of cells the molecules specifiable as Nanney’s
741 extracellular propagators F_N^{\rightarrow} at any instant t may not be specifiable
742 as such at some later instant¹³ $t + \Delta t$.
- 743 (ii) The emergent *telos* or “end” in this theory is the instantaneous, higher-order
744 intrinsic constraint that emerges from proliferating undifferentiated cells
745 (i.e. the multicellular *self*); *not* a *telos* such as the organism’s mature form, a
746 fully differentiated cell, or certain future transcriptional changes to achieve
747 such states (described as “intuitive” in the [introduction](#)), which are logically
748 inconsistent¹⁴ and unjustifiably homuncular.
- 749 (iii) This causally-efficacious, higher-order constraint emerges from the
750 synergistic coupling of lower-order Waddington’s constraints C_W and
751 Nanney’s constraints C_N across the extracellular space S_E .
- 752 • Therefore, under this theory cell differentiation “terminates” (the quotes
753 will be justified below) in any given region S_{E_i} of the extracellular space if
754 a stable or metastable equilibrium is reached where at least one of the two
755 following conditions is true:
- 756 (a) The gradients $\{\vec{\nabla}\Phi_{N_1}, \dots, \vec{\nabla}\Phi_{N_k}\}$ dissipate in S_{E_i} under certain critical
757 values, i.e. $(|\vec{\nabla}\Phi_{N_1}|, \dots, |\vec{\nabla}\Phi_{N_k}|) < (V_{D_1}, \dots, V_{D_k}), (r, \theta, \phi) \in S_{E_i}$ (see
758 question [Q8](#) and [Figure 6B, left](#)).
- 759 • Condition (a) can be reached for example when development significantly
760 changes the morphology of the cells by increasing their surface-to-volume
761 ratio. This is because such increase removes spatial constraints in S_E that
762 facilitate the emergence/maintenance of the gradients.
- 763 • It is thus predictable under this theory a *significant positive correlation*
764 *between the degree of differentiation of a cell and its surface-to-volume ratio*,
765 once controlling for characteristic length (i.e. “unidimensional size”) and
766 also a *significant negative correlation between cell potency/regenerative capacity*
and that ratio.

¹³This exemplifies why the [theoretical definitions and notation](#) had to be developed in instantaneous terms.

¹⁴Since such a *telos* entails the causal power of future events on events preceding them.

767
768
769
770
771
772
773
774
775
776
777
778
779
780
781
782
783
784
785
786
787
788
789

- (b) The gradients $\{\vec{\nabla}\Phi_{N_1}, \dots, \vec{\nabla}\Phi_{N_k}\}$ are unable to constrain Waddington's embodiery F_W in the cells' nuclei because the critical gene products (protein channels/carriers or signal transducers) are non-functional or not expressed, i.e. when the cells become "blind" to the gradients (see question Q8 and Figure 6B, right).
- Condition (b) can be reached when the cell differentiation process represses at some point the expression of the protein channels or carriers necessary for the facilitated diffusion/signal transduction of the *current* Nanney's extracellular propagators $F_N^{\vec{}}$.
 - Importantly, the stability of the equilibrium will depend on the cells' currently expressed phenotype, e.g. an adult multipotent or pluripotent stem cell may differentiate if needed [52] or some differentiated cells may dedifferentiate given certain stimuli [53] (metastable equilibrium), in stark contrast to a fully differentiated neuron (very stable equilibrium).
 - These examples underscore that the *telos* of cell differentiation is not a "fully differentiated" state but, as this theory explains, the instantaneous, intrinsic higher-constraint which is the multicellular organism as a whole. Consequently, the "termination" of cell differentiation should be understood rather as an indefinite-as-long-as-functional stop, or even as apoptosis (see question Q8).
 - The multicellular *telos* described will prevail in ontogeny (and did prevail in evolution) as long as an even higher-order *telos* does not emerge from it (e.g. once a central nervous system develops/evolved).

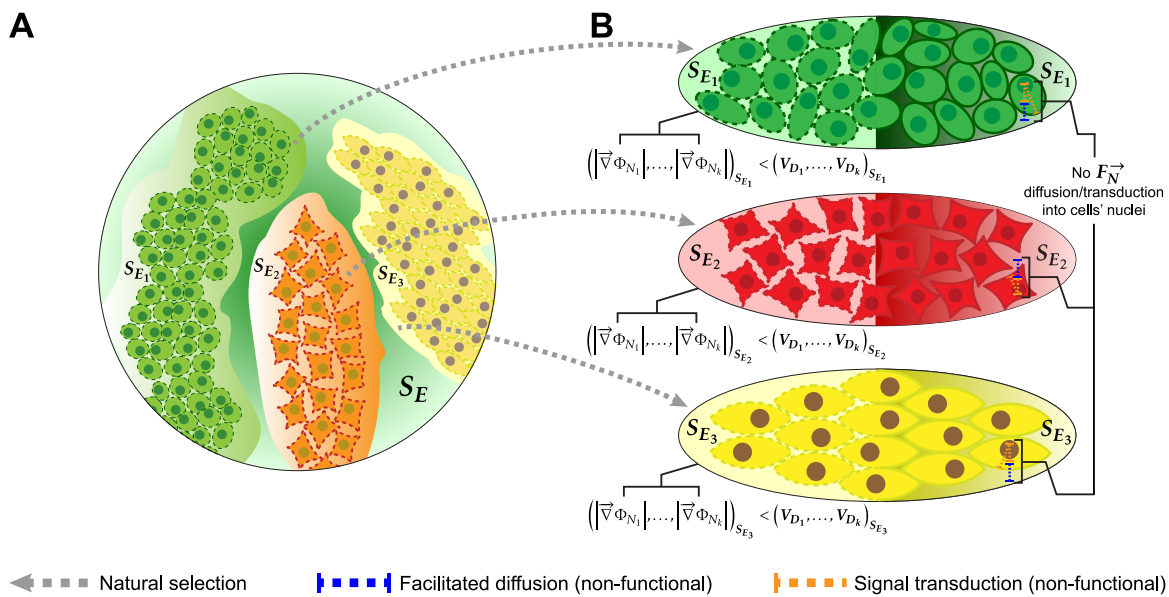


Figure 6: **A:** Cell types/tissues/organs evolve as emergent "blobs" of relatively small $\vec{\nabla}\Phi_N$ magnitude and then are shaped by natural selection (**E**). **B:** Cell differentiation stops when the $\vec{\nabla}\Phi_N$ gradients dissipate (**left**), or when they cannot diffuse/be transduced into the cells' nuclei (**right**).

790 **Part X**
791 **(Evolution)**

The evolutionarily-shaped multicellular *telos*

- 792 • Whereas the causal power of the organism’s mature form—a potential
793 future state—as ontogenetic *telos* is logically inconsistent and only
794 apparent, the assumption that the zygote is a complete developmental
795 blueprint containing all necessary information for the process, as argued in
the [introduction](#), is also untenable.
- 796 • In contrast, ontogeny is, under this theory, an emergent,
797 evolutionarily-shaped and instantaneously-defined (i.e. logically consistent)
798 teleological process. The reason why it intuitively appears to be “directed”
799 to and by the organism’s mature form is that the intrinsic higher-order
800 constraint—the true (instantaneous) *telos* described previously—and the
801 hologenic information content emerging along with it are exerting, instant
802 after instant, efficacious causal power on the ontogenetic process.
- 803 • Although the propagation of constraints within this process (e.g. propagated
804 changes in gene expression) is decomposable into molecular interactions,
805 its “end-directed” causal power (e.g. self-regulation) *is not*. This is because
806 its *telos* is a spontaneous, intrinsic higher-order *constraint* or “dynamical
807 analogue of zero” emergent from lower-order constraints; it cannot be
808 reduced or decomposed into molecular interactions—as the arithmetic zero
809 cannot be divided and for the same fundamental reason—as T. Deacon
810 first argued [46].
- 811 • This is also why hologenic content (and in general any information content,
812 as Deacon has argued as well) is thermodynamically *absent* or constrained:
813 hologenic content is not in the molecular substrates conveying that content
814 anymore than the content of this theory is in integrated circuits, computer
815 displays, paper, or even in the complex neural interactions within the
816 reader’s brain. As described previously in less specific terms, what becomes
817 constrained (i.e. “*absent*”) in the dynamics of the multicellular organism is
818 the content of hologenic information (see question [Q3](#)); the substrates
819 propagating the critical constraints for this change can only then be
820 identified as conveying hologenic information.
- 821 • Evolution has thus selected the content of hologenic information by
822 capturing the lower-order genetic information it is ultimately emergent
823 from, not any particular molecules or molecular interactions as media,
824 which should be regarded in this context as means to the multicellular *telos*,
825 as the etymology indirectly implies. This also implies a trade-off between
826 cell independence and cell phenotypic complexity: the multicellular *telos*
827 offloads regulatory work (i.e. constraints, as described in [Part VI-Evolution](#))
828 the cells were performing individually, allowing them to use that free energy
829 surplus in more complex and differentiated dynamics but also making them
830 more dependent on the multicellular *telos*.

- 831 • In this context, the necessary genetic change from the genome of the cell $U_{(i;t_{U_0})}$ to the genome of the cell $U_{(k;t_M-\Delta t_M)}$ (described
832 in [Part II-Evolution](#)) could well have been significantly smaller—in terms
833 of DNA or protein sequence—than other genetic changes suffered by the
834 eukaryotic ancestors of $U_{(k;t_M-\Delta t_M)}$ while never leaving unicellularity or
835 undifferentiated multicellularity. In general, accounting for substantial
836 differences in the phenotype and its properties¹⁵ given comparatively
837 small genetic changes is bound to be an intractable task if one or more
838 teleodynamic transitions during evolution is/are involved yet ignored.
839
- 840 • In hindsight, the [description](#) for the evolution of cell types, tissues and
841 organs based on initial “blobs” of relative F_N^{\rightarrow} uniformity in S_E together
842 with the predicted positive correlation between degree of cell differentiation
843 and cell surface-to-volume ratio suggest an additional and more specific
844 evolutionary implication.
- 845 • That is, the high surface-to-volume ratio morphology needed for neuron
846 function—and possibly neuron function itself—was only to be expected
847 in the evolution of multicellularity and is only to be expected in
848 multicellular-like life (if any) elsewhere in the Universe, provided no rigid
849 wall (of high relative fitness) impedes the tinkering with substantial increases
850 of the cells’ surface-to-volume ratio, as observable in plants.
- 851 • In turn this caveat—now together with the predicted negative correlation
852 between cell potency and surface-to-volume ratio—suggests that
853 if a multicellular lineage is constrained to always display low cell
854 surface-to-volume ratios, cell potency and regenerative capacity will be
855 higher. All other things being equal, these multicellular lineages should be
856 characterized then by a comparatively lower complexity but also by longer
857 lifespan and more robustness to extrinsic damage (see question [Q5](#)).
858
859

860 The synergy in the coupling of Waddington’s constraints C_W and Nanney’s constraints C_N
861 across S_E described in this theory does not preclude that cell differentiation may display phases
862 dominated by proliferation and others dominated by differentiation itself: whereas significant
863 gradients of Nanney’s extracellular propagators F_N^{\rightarrow} in S_E emerge at some point given enough
864 cell proliferation, it is also true that the exchange of such propagators between the cells and S_E
865 is constrained by the dynamics of facilitated diffusion and/or ligand-receptor binding which,
866 importantly, are saturable. Any representative simulation of cell differentiation according to this
867 theory, however simple, will depend on an accurate modeling of the lower-order dynamical
868 constraints it emerges from.

¹⁵When great, these differences usually involve intrinsically teleological dynamics at a variety of levels, e.g. function, regulation, courtship, or planning.

869 Importantly, this theory also encompasses coenocytic (also commonly called “syncytial”) stages of
870 development, where cell nuclei divide in absence of cytokinesis (observable in some invertebrates
871 such as *Drosophila*). In such stages, Nanney’s extracellular propagators have to be operationally
872 redefined as Nanney’s *extranuclear* propagators, while still maintaining their fundamental defining
873 property: the ability to elicit a change in Nanney’s embodyers F_N inside the nucleus.

874 In terms of results indirectly related to this theory, it must be noted that evidence has already been
875 found for tissue migration across a migration-generated chemokine gradient in zebrafish [54, 55].
876 This finding demonstrates the feasibility of some of the dynamics proposed here, namely
877 eukaryotic cells utilizing certain free energy (available in the spontaneous constraints on diffusion
878 in S_E generated by cell migration/proliferation) as work in their own intrinsic dynamics. These two
879 linked processes—one spontaneous, the other non-spontaneous—exemplify a work cycle as
880 proposed by Stuart Kauffman [56]. What remains to be verified is the synergistic coupling of two
881 (as in this theory) or more lower-order constraint generating systems, as proposed by T. Deacon,
882 into the intrinsic higher-order constraint or multicellular organism described here.

883 Falsifiability

884 Popper's criterion of falsifiability will be met in this paper by providing the three following
885 experimentally-testable predictions:

- 886 1. Under the proposed theory, the gradient $\vec{\nabla}\Phi_N$ in the extracellular space S_E such that
887 $\left|\vec{\nabla}\Phi_N\left(D_{(1;t_D)}, \dots, D_{(n;t_D)}, r, \theta, \phi\right)\right| \geq V_D, (r, \theta, \phi) \in S_E$ is a necessary condition for the
888 emergence of cell differentiation during ontogeny. It follows directly from this proposition
889 that *if undifferentiated stem cells or their differentiating offspring are extracted continuously*
890 *from a developing embryo at the same rate they are proliferating*, then at some instant $t_D + \Delta t$
891 the significant gradient (if any) of Nanney's extracellular propagators in S_E will dissipate by
892 virtue of the Second Law of thermodynamics, reaching everywhere values under the critical
893 value, i.e. $\left|\vec{\nabla}\Phi_N\left(D_{(1;t_D+\Delta t)}, \dots, D_{(n;t_D+\Delta t)}, r, \theta, \phi\right)\right| < V_D, (r, \theta, \phi) \in S_E$. Thus, as long as
894 cells are extracted, *the undifferentiated cells will not differentiate or the once differentiating*
895 *cells will enter an artificially-induced diapause or developmental arrest*. A proper experimental
896 control will be needed for the effect of the cell extraction technique itself (that is, applying
897 it to the embryo but extracting no cells).
- 898 2. *A significant positive correlation will be observed between the overall cell-type-wise dissimilarity*
899 *of Nanney's constraints C_N in an embryo and developmental time*. In practical terms, totipotent
900 cells can be taken from early-stage embryos and divided into separate samples, and for
901 each later developmental time point groups of cells can be taken (ideally according
902 to distinguishable cell types or differentiated regions) from the embryos and treated
903 as separate samples. Then, ChIP-seq on histone H3 modifications and RNA-seq on
904 mRNA can be used to obtain the corresponding *ctalk_non_epi* profile—which represent
905 Nanney's constraints C_N on histone H3 modifications (adjacent to TSSs) as embodiars—for
906 each sample. If the extraction or sectioning technique is able to generate samples for
907 ChIP-seq/RNA-seq with high cell-type specificity and the computational analysis fails to
908 verify the predicted correlation, the theory proposed here should be regarded as falsified.
- 909 3. *If any molecule M (i) is specifiable as a Nanney's extracellular propagator $F_N^{\vec{\nabla}}$ during a certain*
910 *time interval for certain cells of a differentiated multicellular species (see [Corollary #1](#)) and*
911 *(ii) is also synthesized by an unicellular (or undifferentiated multicellular) eukaryote species U*
912 *(e.g. the dinoflagellate *Lingulodinium polyedrum* [57]), then experiments will fail to specify M*
913 *as a Nanney's extracellular propagator $F_N^{\vec{\nabla}}$ for the species U .*

914 Corollaries

915 Described next are some corollaries, hypotheses and predictions (not involving falsifiability) that
916 can be derived from the theory.

917 **1. Nanney's extracellular propagators.** The strongest prediction that follows from the
918 theory is *the existence of Nanney's extracellular propagators F_N^{\rightarrow} in any differentiated*
919 *multicellular species*. Since these propagators are instantaneously defined, their identification
920 should be in the form “molecule M is specifiable as a Nanney's extracellular propagator of
921 the species D in the cell, cell population, or cell type T_j at the developmental time point t
922 (or the differentiation state s)”. This will be verified if, for instance, an experiment shows
923 that the *ctalk_non_epi* profiles in these T_j cell or cells vary significantly when exposed
924 to differential concentrations of M in the extracellular medium. If this is the case, it is
925 also predictable that M will be synthesized by the cells *in vivo* at a relatively constant rate
926 (at least as long as M is specifiable as F_N^{\rightarrow} for them). Importantly, *there is no principle in*
927 *this theory precluding a first messenger molecule M known to elicit transcriptional-rate changes*
928 *(e.g. a well-known morphogen) from being also specifiable as a Nanney's propagator F_W^{\rightarrow} ¹⁶.*
929 In other words, rather than the existence of a previously undescribed molecule, what will
930 be verified is the ability of some membrane-exchangeable molecules to elicit changes in
931 Nanney's constraints C_N (e.g. eliciting changes in histone H3 crosstalk in TSS-adjacent
932 genomic regions *irrespectively* of what the transcriptional rates are) in the cells' nuclei.
933 Note: although the existence of these Nanney's extracellular propagators is a very strong
934 and verifiable prediction, it was not included in the [previous subsection](#) because it is not
935 falsifiable in a strict epistemological sense.

936 **2. Surface-to-volume ratio and the evolution and development of the extracellular**
937 **matrix.** It was proposed earlier ([Part X-Evolution](#)) an important relationship between
938 cell surface-to-volume ratio and the evolution of differentiated multicellularity, in
939 particular between the neuron's high surface-to-volume ratio and the evolution of its
940 function. Importantly, under the predicted relationship between regenerative capacity
941 and surface-to-volume ratio (see [Part X-Ontogeny](#)) neuron-shaped cells are expected to
942 be the most difficult to regenerate. This would have been the (developmental) price to
943 pay for a higher-order, dynamically faster form of multicellular *self* (i.e. higher-order
944 intrinsic constraint) that neurons—whose interconnectivity is underpinned by their high
945 surface-to-volume ratio—make possible. On the other hand glial cells (companions of
946 neurons in the nervous tissue) have a smaller surface-to-volume ratio than neurons so
947 they would support them by constraining to some extent the diffusion flux of Nanney's
948 extracellular propagators F_N^{\rightarrow} in the neurons “effective” extracellular space¹⁷. Notably, the
949 glial cells with the smallest surface-to-volume ratio are ependymal cells, which have been
950 found able to serve as neural stem cells [58]. Since this analysis is based on constraints
951 and not on their specific molecular embodiments, the logic of the neurons and glial cells

¹⁶This dual specifiability is not unlikely, since the synergistic coupling of Waddington's constraints C_W and Nanney's constraints C_N across S_E requires that at least one type of molecular substrates is simultaneously specifiable as Waddington's embodiens F_W and Nanney's embodiens F_N .

¹⁷Understood in this case as the neuroglia plus the neural extracellular matrix.

952 example can be extended to the evolution and development of the extracellular matrix
953 in general. That is, the extracellular matrix was not only shaped by natural selection
954 making it provide the cells structural and biochemical support but also developmental
955 support, understood as fine-tuned differential constraints to the diffusion flux of Nanney's
956 extracellular propagators F_N^{\rightarrow} in S_E . Moreover, I submit that the evolution of this
957 developmental support probably preceded the evolution of all other types of support,
958 given the critical role of the F_N^{\rightarrow} gradients in the emergence and preservation of the
959 multicellular *telos*.

960 **3. Natural developmental arrests or diapauses.** The account for natural
961 diapauses—observable in arthropods [59] and some species of killifish
962 (Cyprinodontiformes) [60]—in this theory follows directly from the description
963 in [Part X-Ontogeny](#). That is, natural diapauses are a metastable equilibrium state
964 characterized by (i) the dissipation of Nanney's extracellular propagators F_N^{\rightarrow} in S_E under
965 certain critical values (e.g. if some factor inhibits cell proliferation) or (ii) the inability of
966 these gradients to constrain Waddington's embodyers F_W in the cells' nuclei because the
967 critical gene products (protein channels/carriers or signal transducers) are non-functional
968 or not expressed. For example, if in some organism the function of the gene products
969 critical for the facilitated diffusion/signal transduction of the current F_N^{\rightarrow} is temperature
970 dependent, then at that time development will enter a diapause given certain thermal
971 conditions and resume when those conditions are lost.

972 **4. F_N^{\rightarrow} gradients and tissue regeneration.** Whereas the scope of the theory
973 is the dynamics of cell differentiation and the evolution of differentiated
974 multicellularity, it may provide some hints about other developmental processes
975 such as tissue regeneration after extrinsic damage. For instance, I hypothesize
976 that an important constraint driving the regenerative response to wounds
977 (e.g. a cut in the skin) is the gradient $\left| \vec{\nabla} \Phi_N \left(D_{(1;t_{\text{wound}})}, \dots, D_{(n;t_{\text{wound}})}, r, \theta, \phi \right) \right| \gg$
978 $\left| \vec{\nabla} \Phi_N \left(D_{(1;t_{\text{wound}}-\Delta t)}, \dots, D_{(n;t_{\text{wound}}-\Delta t)}, r, \theta, \phi \right) \right|$, $(r, \theta, \phi) \in S_E$ generated by the wound
979 itself. This is because a cut creates an immediate, significant gradient at the wound
980 edges (evidence has been already found for extracellular H_2O_2 gradients mediating wound
981 detection in zebrafish [61]). If relevant variables (such as F_N^{\rightarrow} diffusivity in the extracellular
982 space S_E , see [Corollary #2](#)) prevent this gradient from dissipating quickly, it should
983 contribute to a developmental regenerative response as it dissipates gradually. If different
984 tissues of the same multicellular individual are compared, a significant negative correlation
985 should be observable between the regenerative capacity after injury in a tissue and
986 the average cell surface-to-volume ratio in that tissue, once controlling for average cell
987 characteristic length.

988 **5. Effects of microgravity on development.** In the last few decades a number of abnormal
989 effects of microgravity on development-related phenomena—including mammal tissue
990 culture [62], plant growth [63], human gene expression [64], cytoskeleton organization and
991 general embryo development ([65] and references therein)—have been described. A general
992 explanation proposed for these effects is that microgravity introduces a significant degree of
993 mechanical perturbation on critical structures for cells and tissues which as a whole would

994 be the “gravity sensors” [66]. Without dismissing these structural perturbations as relevant,
995 I suggest that a key perturbation on development elicitable by microgravity is a significant
996 alteration—with respect to standard gravity—of the instantaneous $F_{\vec{N}}$ distribution in
997 the extracellular space S_E . This could be explained in turn by changes in the diffusion
998 dynamics (as evidence for changes in the diffusion of miscible fluids suggest [67]) and/or a
999 significant density difference between the extracellular space S_E and the cells.

1000 **6. Why plant seeds need water.** It is a well-known fact that plant seeds only need certain
1001 initial water intake to be released from dormancy and begin to germinate with no further
1002 extrinsic support. Whereas this specific requirement of water has been associated to embryo
1003 expansion and metabolic activation of the seeds [68, 69], I submit that it is also associated
1004 to the fundamental need for a medium in S_E where the critical $F_{\vec{N}}$ gradients can emerge.
1005 This is because such gradients are in turn required for the intrinsic regulation of the
1006 asymmetric divisions already shown critical for cell differentiation in plants [70].

1007 **Concluding remarks**

1008 The analysis conducted to search for the theoretical proof of principle in this work encompassed
1009 two relevant simplifications or approximations: gene expression levels were represented
1010 theoretically by instantaneous transcription rates, which in turn were approximated by mRNA
1011 abundance in the analysis. These steps were justified since (i) the correlation between gene
1012 expression and mRNA abundance has been clearly established as positive and significant
1013 in spite of the limitations of the techniques available [71, 72], (ii) if gene expression can be
1014 accurately expressed as a linear transformation of mRNA abundance as the control variable, the
1015 *ctalk_non_epi* profiles will remain unchanged (see details in [Materials and Methods](#)) and, (iii) the
1016 association between *ctalk_non_epi* profiles and cell differentiation states was robust with respect
1017 to these simplifications and approximations as shown in the [Results](#).

1018 If the theory advanced here is ever tested and resists falsification attempts consistently,
1019 further research will be needed to identify the cell-and-instant-specific Nanney's extracellular
1020 propagators F_N^{\rightarrow} at least for each multicellular model organism, and also to identify the
1021 implications (if any) of this theory on other developmental processes such as aging or diseases
1022 such as cancer. Also, more theoretical development will be needed to quantify the capacity and
1023 classify the content of hologenic information that emerges along with cell differentiation.

1024 On the other hand, I wish to underscore that the critique of the epigenetic landscape approach
1025 presented in the [introduction](#) (in terms of its assumed ability to explain the self-regulatory
1026 dynamics of cell differentiation) is completely independent from a potential falsification of
1027 the theory. Even that being the case, I argue that if future research keeps on elucidating the
1028 mechanisms propagating changes in gene expression to an arbitrarily high level of detail—while
1029 failing to recognize that the constraints that truly regulate changes¹⁸ must be explicitly
1030 uncorrelated yet coupled to the constraints that propagate those changes—advances in the
1031 fundamental understanding of the evolution and self-regulatory dynamics of differentiated
1032 multicellularity will not be significant.

1033 What underpins this view is that scientifically tenable (i.e. instantaneous) teleological dynamics
1034 in nature—unless we are still willing to talk about intrinsically teleological concepts like
1035 function, regulation, agency, courtship or planning in all fields of biology while holding they
1036 are fundamentally meaningless—can emerge only from lower-order systems that are *explicitly*
1037 *uncorrelated* with respect to each other in terms of their dynamics. Furthermore, the only way
1038 such requisite can be fulfilled is that an intrinsic higher-order constraint emerges from the
1039 synergistic coupling of lower-order *constraint* generating systems, as Terrence Deacon first
1040 proposed. Whereas this thermodynamically spontaneous, intrinsic constraint or dynamical *telos*
1041 is dependent on molecular substrates embodying it at any instant, these substrates can be added,
1042 replaced or even dispensed with at any instant as long as the *telos* is preserved. For all these
1043 reasons, the differentiated multicellular organism described in this theory (and any living system
1044 in general) is no mechanism or machine of any type (e.g. autopoietic [73])—interconnecting in
1045 this case a eukaryotic cell population—for mechanisms and machines *are definable by the explicit*
1046 *correlation* of their components in dynamical terms.

¹⁸Whatever those constraints are if not the ones described in this theory.

1047 Thus, the emergence of differentiated multicellularity throughout evolution and in every successful
1048 ontogenetic process has been—and still is—the emergence of unprecedented, constraint-based,
1049 thermodynamic *selves* in the natural world; *selves* which no machine or mechanism could
1050 ever be.

1051 **Materials and Methods**

1052 **Data collection**

1053 The genomic coordinates of all annotated RefSeq TSSs for the hg19 (*Homo sapiens*),
1054 mm9 (*Mus musculus*), and dm3 (*Drosophila melanogaster*) assemblies were downloaded from the
1055 UCSC database. Publicly available tandem datafiles of ChIP-seq¹⁹ on histone H3 modifications
1056 and RNA-seq²⁰ for each analyzed cell sample in each species were downloaded from the
1057 ENCODE, modENCODE or NCBI's SRA databases [74, 75, 76, 77, 78, 79, 80].

1058 The criteria for selecting cell type/cell sample datasets in each species was (i) excluding those
1059 associated to abnormal karyotypes and (ii) among the remaining datasets, choosing the group
1060 that maximizes the number of specific histone H3 modifications shared. Under these criteria, the
1061 comprised cell type/sample datasets in this work were thus:

1062
1063 ***H. sapiens*** 6 cell types: HSMM (skeletal muscle myoblasts), HUVEC (umbilical
1064 vein endothelial cells), NHEK (epidermal keratinocytes), GM12878
1065 (B-lymphoblastoids), NHLF (lung fibroblasts) and H1-hESC (embryonic stem
1066 cells).

1067 9 histone H3 modifications: H3K4me1, H3K4me2, H3K4me3, H3K9ac,
1068 H3K9me3, H3K27ac, H3K27me3, H3K36me3, and H3K79me2.

1069 ***M. musculus*** 5 cell types: 8-weeks-adult heart, 8-weeks-adult liver, E14-day0 (embryonic
1070 stem cells after zero days of differentiation), E14-day4 (embryonic stem cells
1071 after four days of differentiation), and E14-day6 (embryonic stem cells after
1072 six days of differentiation).

1073 5 histone H3 modifications: H3K4me1, H3K4me3, H3K27ac, H3K27me3, and
1074 H3K36me3.

1075 ***D. melanogaster*** 9 cell samples: 0-4h embryos, 4-8h embryos, 8-12h embryos, 12-16h embryos,
1076 16-20h embryos, 20-24h embryos, L1 larvae, L2 larvae, and pupae.

1077 6 histone H3 modifications: H3K4me1, H3K4me3, H3K9ac, H3K9me3,
1078 H3K27ac, and H3K27me3.

1079
1080 See [Supplementary Information](#) for the datafile lists in detail.

¹⁹Comprising 1×36 bp, 1×50 bp, and 1×75 bp reads, depending on the data series (details available via GEO accession codes listed in [Supplementary Information](#)).

²⁰Comprising 1×36 bp, 1×100 bp, and 2×75 bp reads, depending on the data series (details available via GEO accession codes listed in [Supplementary Information](#)).

1081 **ChIP-seq read profiles and normalization**

1082 The first steps in the EFilter algorithm by Kumar *et al.*—which predicts mRNA levels
1083 in log-FPKM (fragments per transcript kilobase per million fragments mapped) with high
1084 accuracy ($R \sim 0.9$) [21]—were used to generate ChIP-seq read signal profiles for the histone H3
1085 modifications data. Namely, (i) dividing the genomic region from 2 kbp upstream to 4 kbp
1086 downstream of each TSS into 30 200-bp-long bins, in each of which ChIP-seq reads were later
1087 counted; (ii) dividing the read count signal for each bin by its corresponding control (Input/IgG)
1088 read density to minimize artifactual peaks; (iii) estimating this control read density within a
1089 1-kbp window centered on each bin, if the 1-kbp window contained at least 20 reads. Otherwise,
1090 a 5-kbp window, or else a 10-kbp window was used if the control reads were less than 20. When
1091 the 10-kbp length was insufficient, a pseudo-count value of 20 reads per 10kbp was set as the
1092 control read density. This implies that the denominator (i.e. control read density) is at least 0.4
1093 reads per bin. When replicates were available, the measure of central tendency used was the
1094 median of the replicate read count values.

1095 **ChIP-seq read count processing**

1096 When the original format was SRA, each datafile was pre-processed with standard tools in the
1097 pipeline

```
1098  
1099 fastq-dump → bwa aln [genome.fa] → bwa samse → samtools view -bS -F 4  
1100 → samtools sort → samtools index
```

1101 to generate its associated BAM and BAI files. Otherwise, the tool

```
1102  
1103 bedtools multicov -bams [file.bam] -bed [bins_and_controlwindows.bed]
```

1104 was applied (excluding failed-QC reads and duplicate reads by default) directly on the
1105 original BAM²¹ file to generate the corresponding read count file in BED format.
1107

1108 **RNA-seq data processing**

1109 The processed data were mRNA abundances in FPKM at RefSeq TSSs. When the original format
1110 was GTF (containing already FPKM values, as in the selected ENCODE RNA-seq datafiles
1111 for *H. sapiens*), those values were used directly in the analysis. When the original format was
1112 SAM, each datafile was pre-processed by first sorting it to generate then a BAM file using
1113 `samtools view -bS`. If otherwise the original format was BAM, mRNA levels at RefSeq TSSs
1114 were then calculated with FPKM as unit using *Cufflinks* [81] directly on the original file with the
1115 following options:
1116

²¹The BAI file is required implicitly.

1117 -GTF-guide <reference_annotation.(gtf/gff)>
1118 -frag-bias-correct <genome.fa>
1119 -multi-read-correct■
1120

1121 When the same TSS (i.e. same genomic coordinate and strand) displayed more than one identified
1122 transcript in the *Cufflinks* output, the respective FPKM values were added. Also, when replicates
1123 were available the measure of central tendency used was the median of the replicate FPKM
1124 values.

1125 Preparation of data input tables

1126 For each of the three species, all TSS_{def}—defined as those TSSs with measured mRNA
1127 abundance (i.e. FPKM > 0) in all cell types/cell samples—were determined. The number of TSS_{def}
1128 found for each species were $N_{\text{TSS}_{\text{def}}}(\textit{Homo sapiens}) = 14,742$; $N_{\text{TSS}_{\text{def}}}(\textit{Mus musculus}) = 16,021$;
1129 and $N_{\text{TSS}_{\text{def}}}(\textit{Drosophila melanogaster}) = 11,632$. Then, for each cell type/cell sample, 30 genomic
1130 bins were defined and denoted by the distance (in bp) between their 5'-end and their respective
1131 TSS_{def} genomic coordinate: “-2000”, “-1800”, “-1600”, “-1400”, “-1200”, “-1000”, “-800”,
1132 “-600”, “-400”, “-200”, “0” (TSS_{def} or ‘+1’), “200”, “400”, “600”, “800”, “1000”, “1200”,
1133 “1400”, “1600”, “1800”, “2000”, “2200”, “2400”, “2600”, “2800”, “3000”, “3200”, “3400”,
1134 “3600”, and “3800”. Then, for each cell type/cell sample, a ChIP-seq read signal was computed
1135 for all bins in all TSS_{def} genomic regions (e.g. in the “-2000” bin of the *Homo sapiens* TSS with
1136 RefSeq ID: NM_001127328, H3K27ac₋₂₀₀₀ = 4.68 in H1-hESC stem cells). Data input tables,
1137 with n_m being the number of histone H3 modifications comprised, were generated following this
1138 structure of rows and columns²²:

	H3[1] ₋₂₀₀₀	...	H3[n_m] ₋₂₀₀₀	...	H3[1] ₃₈₀₀	...	H3[n_m] _{3,800}	FPKM
1								
⋮								
$N_{\text{TSS}_{\text{def}}}$								

1140 The tables were written then to these data files:

1141 ***H. sapiens***: Hs_Gm12878.dat, Hs_H1hesc.dat, Hs_Hsmm.dat, Hs_Huvec.dat,
1142 Hs_Nhek.dat, Hs_Nhlf.dat■

1143 ***M. musculus***: Mm_Heart.dat, Mm_Liver.dat, Mm_E14-d0.dat, Mm_E14-d4.dat,
1144 Mm_E14-d6.dat■

1145 ***D. melanogaster***: Dm_E0-4.dat, Dm_E4-8.dat, Dm_E8-12.dat, Dm_E12-16.dat,
1146 Dm_E16-20.dat, Dm_E20-24.dat, Dm_L1.dat, Dm_L2.dat,
1147 Dm_Pupae.dat■

²²For reference, additional columns were appended in the generated .dat files after the FPKM column with the chromosome, position, strand and RefSeq ID of each TSS_{def}.

1148 Computation of *ctalk_non_epi* profiles

1149 If the variables X_j (representing the signal for histone H3 modification X in the genomic bin
 1150 $j \in \{-2000, \dots, 3800\}$), Y_k (representing the signal for histone H3 modification Y in the
 1151 genomic bin $k \in \{-2000, \dots, 3800\}$) and Z (representing FPKM values) are random variables,
 1152 then the covariance of X_j and Y_k can be decomposed directly in terms of their linear relationship
 1153 with Z as the sum

$$\text{Cov}(X_j, Y_k) = \underbrace{\frac{\text{Cov}(X_j, Z)\text{Cov}(Y_k, Z)}{\text{Var}(Z)}}_{\substack{\text{covariance of } X_j \text{ and } Y_k \\ \text{resulting from their} \\ \text{linear relationship with } Z}} + \underbrace{\text{Cov}(X_j, Y_k|Z)}_{\substack{\text{covariance of } X_j \text{ and } Y_k \\ \text{orthogonal to } Z}}, \quad (1)$$

1154 where the second summand $\text{Cov}(X_j, Y_k|Z)$ is the partial covariance between X_j and Y_k given Z .
 1155 It is easy to see that $\text{Cov}(X_j, Y_k|Z)$ is a local approximation of Nanny's constraints C_N on
 1156 histone H3 modifications, as anticipated in the preliminary theoretical definitions²³. To make the
 1157 *ctalk_non_epi* profiles comparable however, $\text{Cov}(X_j, Y_k|Z)$ values have to be normalized²⁴ by the
 1158 standard deviations of the residuals of X_j and Y_k with respect to Z . In other words, the partial
 1159 correlation $\text{Cor}(X_j, Y_k|Z)$ values were needed. Nevertheless, a correlation value does not have a
 1160 straightforward interpretation, whereas its square—typically known as *coefficient of determination*,
 1161 *effect size of the correlation*, or simply r^2 —does: it represents the relative (i.e. fraction of) variance
 1162 of one random variable explained by the other. For this reason, $\text{Cor}(X_j, Y_k|Z)^2$ was used to
 1163 represent the strength of the association, and then multiplied by the sign of the correlation to
 1164 represent the direction of the association. Thus, after \log_2 -transforming the X_j , Y_k and Z data,
 1165 each pairwise combination of bin-specific histone H3 modifications $\{X_j, Y_k\}$ contributed with
 1166 the value

$$\text{ctalk_non_epi}(X_j, Y_k) = \underbrace{\text{sgn}(\text{Cor}(X_j, Y_k|Z))}_{\substack{\text{partial correlation} \\ \text{sign} \in \{-1, 1\}}} \underbrace{(\text{Cor}(X_j, Y_k|Z))^2}_{\substack{\text{partial correlation} \\ \text{strength} \in [-1, 1]}}. \quad (2)$$

1167 This implies that for each pairwise combination of histone H3 modifications $\{X, Y\}$, there
 1168 are 30 (bins for X) \times 30 (bins for Y) = 900 (bin-combination-specific *ctalk_non_epi* values). To
 1169 increase the robustness of the analysis against the departures of the actual nucleosome
 1170 distributions from the 30 \times 200-bp bins model, the values were then sorted in descending
 1171 order and placed in a 900-tuple.

²³A straightforward corollary is that Waddington's constraints C_W can in turn be approximated locally by $\frac{\text{Cov}(X_j, Z)\text{Cov}(Y_k, Z)}{\text{Var}(Z)}$.

²⁴At the cost of losing the sum decomposition property, which was used here for explanatory purposes.

1172 For a cell type/cell sample from a species with data for n_m histone H3 modifications,
1173 e.g. $n_m(\textit{Mus musculus}) = 5$, the length of the final *ctalk_non_epi* profile comprising all
1174 possible $\{X, Y\}$ combinations would be ${}^{n_m}C_2 \times 900$. However, a final data filtering
1175 was performed.

1176 The justification for this additional filtering was that some pairwise partial
1177 correlation values were expected a priori to be strong and significant, which was
1178 later confirmed. Namely, (i) those involving the same histone H3 modification in
1179 the same amino acid residue (e.g. $\text{Cor}(\text{H3K9ac}_{-200}, \text{H3K9ac}_{-400}|\text{FPKM}) > 0$;
1180 $\text{Cor}(\text{H3K4me3}_{-200}, \text{H3K4me3}_{-200}|\text{FPKM}) = 1$), (ii) those involving a
1181 different type of histone H3 modification in the same amino acid residue
1182 (e.g. $\text{Cor}(\text{H3K27ac}_{-800}, \text{H3K27me3}_{-600}|\text{FPKM}) < 0$), and (iii) those involving
1183 the same type of histone H3 modification in the same amino acid residue
1184 (e.g. $\text{Cor}(\text{H3K4me2}_{-400}, \text{H3K4me3}_{-400}|\text{FPKM}) > 0$) in part because ChIP-antibody
1185 cross reactivity has been shown able to introduce artifacts on the accurate assessment of
1186 some histone-crosstalk associations [22, 23]. For these reasons, in each species all pairwise
1187 combinations of histone H3 modifications involving the same amino acid residue were then
1188 identified as “trivial” and excluded from the *ctalk_non_epi* profiles construction. E.g., since
1189 for *Mus musculus* the comprised histone modifications were H3K4me1, H3K4me3, H3K27ac,
1190 H3K27me3, and H3K36me3 ($n_m = 5$), the pairwise combinations H3K4me1-H3K4me3 and
1191 H3K27ac-H3K27me3 were filtered out. Therefore, the length of the *Mus musculus ctalk_non_epi*
1192 profiles was $({}^5C_2 - 2) \times 900 = 7,200$.

1193 **Statistical significance assessment**

1194 The statistical significance of the partial correlation $\text{Cor}(X_j, Y_k|Z)$ values, necessary for
1195 constructing the *ctalk_non_epi* profiles, was estimated using Fisher’s z-transformation [82]. Under
1196 the null hypothesis $\text{Cor}(X_j, Y_k|Z) = 0$ the statistic $z = \sqrt{N_{\text{TSS}_{\text{def}}} - |Z| - 3} \frac{1}{2} \ln\left(\frac{1 + \text{Cor}(X_j, Y_k|Z)}{1 - \text{Cor}(X_j, Y_k|Z)}\right)$,
1197 where $N_{\text{TSS}_{\text{def}}}$ is the sample size and $|Z| = 1$ (i.e. one control variable), follows asymptotically
1198 a $N(0, 1)$ distribution. The p-values can be then computed easily using the $N(0, 1)$
1199 probability function.

1200 Multiple comparisons correction of the p-values associated to each *ctalk_non_epi* profile was
1201 performed using the Benjamini-Yekutieli method [83]. The parameter used was the number of all
1202 possible²⁵ comparisons: $({}^{n_m \times 30}C_2)$. From the resulting q-values associated to each *ctalk_non_epi*
1203 profile an empirical cumulative distribution was obtained, which in turn was used to compute
1204 a threshold t . The value of t was optimized to be the maximum value such that within the
1205 q-values smaller than t is expected less than 1 false-positive partial correlation. Consequently,
1206 if $\text{q-value}[i] \geq t$ then the associated partial correlation value was identified as not significant
1207 (i.e. zero) in the respective *ctalk_non_epi* profile.

²⁵Before excluding “trivial” pairwise combinations of histone H3 modifications, to further increase the conservativeness of the correction.

1208 **Unsupervised hierarchical clustering of *ctalk_non_epi* and mRNA** 1209 **abundance profiles**

1210 The goal of this step was to evaluate the significant *ctalk_non_epi*-profile clusters—if any—in
1211 the phenograms (i.e. “phenotypic similarity dendrograms”) obtained from unsupervised
1212 hierarchical clustering analyses (unsupervised HCA). For each species, the analyses were
1213 conducted on (i) the *ctalk_non_epi* profiles of each cell type/sample (**Figure 2A, 2C, and 2E**)
1214 and (ii) the \log_2 -transformed FPKM profiles (i.e mRNA abundance) of each cell
1215 type/sample (**Figure 2B, 2D, and 2F**). Important to the HCA technique is the choice of a
1216 metric (for determining the distance between any two profiles) and a cluster-linkage method (for
1217 determining the distance between any two clusters).

1218 Different ChIP-seq antibodies display differential binding affinities (with respect to different
1219 epitopes or even the same epitope, depending on the manufacturer) that are intrinsic and
1220 irrespective to the biological phenomenon of interest. For this reason, comparing directly
1221 the strengths (i.e. magnitudes) in the *ctalk_non_epi* profiles (e.g. using Euclidean distance as
1222 metric) is to introduce significant biases in the analysis. In contrast, the “correlation distance”
1223 metric—customarily used for comparing gene expression profiles—defined between any two
1224 profiles $pro[i], pro[j]$ as

$$d_r(pro[i], pro[j]) = 1 - \text{Cor}(pro[i], pro[j]) \quad (3)$$

1225 compares instead the “shape” of the profiles²⁶, hence it was the metric used here. On the other
1226 hand, the cluster-linkage method chosen was the “average” method or UPGMA (Unweighted Pair
1227 Group Method with Arithmetic Mean) in which the distance $D(A, B)$ between any clusters A and
1228 B is defined as

$$D(A, B) = \frac{1}{|A||B|} \sum_{\substack{pro[k] \in A \\ pro[l] \in B}} d_r(pro[k], pro[l]), \quad (4)$$

1229 that is, the mean of all distances $d_r(pro[k], pro[l])$ such that $pro[k] \in A$ and $pro[l] \in B$ (this
1230 method was chosen because it has been shown to yield the highest cophenetic correlation values
1231 when using the “correlation distance” metric [84]). Cluster statistical significance was assessed as
1232 *au* (approximately unbiased) and *bp* (bootstrap probability) significance scores by nonparametric
1233 bootstrap resampling using the *Pvclust* [29] add-on package for the *R* software [85]. The number
1234 of bootstrap replicates in each analysis was 10,000.

²⁶ As a consequence of what was highlighted previously, the “correlation distance” metric is also invariant under linear transformations of the profiles.

1235 Suitability of FPKM as unit of mRNA abundance

1236 Previous research has pinpointed that FPKM may not always be an adequate unit of transcript
1237 abundance in differential expression studies. It was shown that, if transcript size distribution
1238 varies significantly among the samples, FPKM/RPKM²⁷ will introduce biases. For this reason
1239 another abundance unit TPM (transcripts per million)—which is a linear transformation of the
1240 FPKM value for each sample—was proposed to overcome the limitation [86]. However, this issue
1241 was not a problem for this study.

1242 This is because partial correlation, used to construct the *ctalk_non_epi* profiles later
1243 subject to HCA, is invariant under linear transformations of the control variable Z
1244 (i.e. $\text{Cor}(X_j, Y_k|Z) = \text{Cor}(X_j, Y_k|aZ + b)$ for any two scalars $\{a, b\}$). Importantly, this property
1245 also implies that *ctalk_non_epi* profiles are controlling not only for mRNA abundance but also
1246 for any other biological variable displaying a strong linear relationship with mRNA abundance
1247 (e.g. chromatin accessibility represented by DNase I hypersensitivity, as shown in [22]). Similarly,
1248 the unsupervised hierarchical clustering of mRNA abundance profiles is invariant under linear
1249 transformations of the profiles, since $\text{Cor}(Z_i, Z_j) = \text{Cor}(aZ_i + b, cZ_j + d)$ provided $ac > 0$.

²⁷Reads per transcript kilobase per million fragments mapped.

1250 **Acknowledgements**

1251 I wish to thank the following people:

- 1252 • John Tyler Dodge, horn soloist at the *Orquesta Filarmónica de Santiago*, for reviewing most
1253 of the English in the first complete draft of this paper and his valuable questions, which
1254 pushed me to the limit of my abilities in the purpose of making this paper self-explanatory.
- 1255 • Kenneth M. Weiss and José M. Neto for reviewing this manuscript and their valuable
1256 questions.
- 1257 • Alejandro Maass for his interest in this work and his valuable questions.
- 1258 • Miguel Allende, director of the FONDAP Center for Genome Regulation (see details in the
1259 institutional acknowledgements below).
- 1260 • My anonymous colleagues who reviewed the grant proposal on behalf of FONDECYT.

1261

1262 Also, I wish to thank the following institutions:

- 1263 • The National Fund for Scientific and Technological Development (FONDECYT, Chile) for
1264 the postdoctoral grant (see details in [Funding](#)).
- 1265 • Universidad Andrés Bello and its Faculty of Biological Sciences for sponsoring my
1266 postdoctoral grant proposal to FONDECYT.
- 1267 • The FONDAP Center for Genome Regulation (CGR, Chile) for generously granting me a
1268 workplace for more than a year and giving me the opportunity to share some preliminary
1269 results of this work with other colleagues at the CGR.
- 1270 • The National Laboratory for High Performance Computing (NLHPC, Chile) for providing
1271 me with a free academic account, which helped me carry out efficiently most of the
1272 computational analyses described in this paper.
- 1273 • The *Math^{omics}* Lab (Chile), for kindly helping me with the setup of my NLHPC account.

1274 **Additional information**

1275 No institution (including the funder) or person other than the author had any role in
1276 study conception, design, publicly-available data collection, computational analysis, theory
1277 development, paper writing, or the decision to submit this preprint to bioRxiv.

1278 **Copyright**

1279 The copyright holder for this preprint is the author. It is made made available under the
1280 Creative Commons Attribution 4.0 International License. To view a copy of this license, visit
1281 <http://creativecommons.org/licenses/by/4.0/>.
1282



1284 **Funding**

	Funder	Grant reference number	Author
1285	National Fund for Scientific and Technological Development (FONDECYT)	3140328	Felipe A. Veloso

References

1286

1287

1288

1289

1290

1291

1292

1293

1294

1295

1296

1297

1298

1299

1300

1301

1302

1303

1304

1305

1306

1307

1308

1309

1310

1311

1312

1313

1314

1315

1316

1317

1318

1319

1320

- [1] Slack JMW (2002) Timeline: Conrad Hal Waddington: the last renaissance biologist? *Nat Rev Genet* 3: 889–895. doi: [10.1038/nrg933](https://doi.org/10.1038/nrg933).
- [2] Waddington CH (1957) *The strategy of the genes: a discussion of some aspects of theoretical biology*. London: Allen & Unwin.
- [3] Wolffe AP (1999) Epigenetics: Regulation through repression. *Science* 286: 481–486. doi: [10.1126/science.286.5439.481](https://doi.org/10.1126/science.286.5439.481).
- [4] Bonasio R, Tu S, Reinberg D (2010) Molecular signals of epigenetic states. *Science* 330: 612–6. doi: [10.1126/science.1191078](https://doi.org/10.1126/science.1191078).
- [5] Kamakura M (2011) Royalactin induces queen differentiation in honeybees. *Nature* 473: 478–483. doi: [10.1038/nature10093](https://doi.org/10.1038/nature10093).
- [6] Fraser P (2010). Defining epigenetics. Interviews by G. Riddihough. *Science* [Video podcast] 00:05:34–00:05:47. URL <http://videolab.sciencemag.org/featured/650920373001/1>.
- [7] Orphanides G, Reinberg D (2002) A unified theory of gene expression. *Cell* 108: 439–451. doi: [10.1016/s0092-8674\(02\)00655-4](https://doi.org/10.1016/s0092-8674(02)00655-4).
- [8] Li G, Reinberg D (2011) Chromatin higher-order structures and gene regulation. *Current Opinion in Genetics & Development* 21: 175–186. doi: [10.1016/j.gde.2011.01.022](https://doi.org/10.1016/j.gde.2011.01.022).
- [9] Cope NF, Fraser P, Eski CH (2010) The yin and yang of chromatin spatial organization. *Genome Biol* 11: 204. doi: [10.1186/gb-2010-11-3-204](https://doi.org/10.1186/gb-2010-11-3-204).
- [10] Ralston A, Shaw K (2008) Gene expression regulates cell differentiation. *Nat Educ* 1: 127. URL <http://www.nature.com/scitable/topicpage/gene-expression-regulates-cell-differentiation-931>.
- [11] Berger SL, Kouzarides T, Shiekhattar R, Shilatifard A (2009) An operational definition of epigenetics. *Genes & Development* 23: 781–783. doi: [10.1101/gad.1787609](https://doi.org/10.1101/gad.1787609).
- [12] Reinberg D (2010). Defining epigenetics. Interviews by G. Riddihough. *Science* [Video podcast] 00:01:25–00:01:35. URL <http://videolab.sciencemag.org/featured/650920373001/1>.
- [13] Arnone MI, Davidson EH (1997) The hardwiring of development: organization and function of genomic regulatory systems. *Development* 124: 1851–64.
- [14] Maduro MF (2010) Cell fate specification in the *c. elegans* embryo. *Dev Dyn* 239: 1315–29. doi: [10.1002/dvdy.22233](https://doi.org/10.1002/dvdy.22233).
- [15] Warner DA, Shine R (2008) The adaptive significance of temperature-dependent sex determination in a reptile. *Nature* 451: 566–568. doi: [10.1038/nature06519](https://doi.org/10.1038/nature06519).
- [16] Power ML, Schulkin J (2013) Maternal regulation of offspring development in mammals is an ancient adaptation tied to lactation. *Applied & Translational Genomics* 2: 55–63. doi: [10.1016/j.atg.2013.06.001](https://doi.org/10.1016/j.atg.2013.06.001).

- 1321 [17] Ladewig J, Koch P, Brüstle O (2013) Leveling waddington: the emergence of direct
1322 programming and the loss of cell fate hierarchies. *Nature Reviews Molecular Cell Biology* 14:
1323 225–236. doi: [10.1038/nrm3543](https://doi.org/10.1038/nrm3543).
- 1324 [18] Nanney DL (1958) Epigenetic control systems. *Proceedings of the National Academy of*
1325 *Sciences* 44: 712–717. doi: [10.1073/pnas.44.7.712](https://doi.org/10.1073/pnas.44.7.712).
- 1326 [19] Huang S (2012) The molecular and mathematical basis of waddington's epigenetic landscape:
1327 a framework for post-darwinian biology? *Bioessays* 34: 149–57. doi: [10.1002/bies.201100031](https://doi.org/10.1002/bies.201100031).
- 1328 [20] Losick R, Desplan C (2008) Stochasticity and cell fate. *science* 320: 65–68.
- 1329 [21] Kumar V, Muratani M, Rayan NA, Kraus P, Lufkin T, et al. (2013) Uniform, optimal signal
1330 processing of mapped deep-sequencing data. *Nat Biotechnol* 31: 615–622. doi:
1331 [10.1038/nbt.2596](https://doi.org/10.1038/nbt.2596).
- 1332 [22] Lasserre J, Chung HR, Vingron M (2013) Finding associations among histone modifications
1333 using sparse partial correlation networks. *PLoS Comput Biol* 9: e1003168. doi:
1334 [10.1371/journal.pcbi.1003168](https://doi.org/10.1371/journal.pcbi.1003168).
- 1335 [23] Peach SE, Rudomin EL, Udeshi ND, Carr SA, Jaffe JD (2012) Quantitative assessment of
1336 chromatin immunoprecipitation grade antibodies directed against histone modifications
1337 reveals patterns of co-occurring marks on histone protein molecules. *Mol Cell Proteomics* 11:
1338 128–37. doi: [10.1074/mcp.M111.015941](https://doi.org/10.1074/mcp.M111.015941).
- 1339 [24] Schwammle V, Aspalter CM, Sidoli S, Jensen ON (2014) Large scale analysis of co-existing
1340 post-translational modifications in histone tails reveals global fine structure of cross-talk.
1341 *Molecular & Cellular Proteomics* 13: 1855–1865. doi: [10.1074/mcp.o113.036335](https://doi.org/10.1074/mcp.o113.036335).
- 1342 [25] Zheng Y, Sweet SMM, Popovic R, Martinez-Garcia E, Tipton JD, et al. (2012) Total kinetic
1343 analysis reveals how combinatorial methylation patterns are established on lysines 27 and
1344 36 of histone h3. *Proc Natl Acad Sci U S A* 109: 13549–54. doi: [10.1073/pnas.1205707109](https://doi.org/10.1073/pnas.1205707109).
- 1345 [26] White KP (1999) Microarray analysis of *Drosophila* development during metamorphosis.
1346 *Science* 286: 2179–2184. doi: [10.1126/science.286.5447.2179](https://doi.org/10.1126/science.286.5447.2179).
- 1347 [27] Cantera R, Ferreira MJ, Aransay AM, Barrio R (2014) Global gene expression shift during
1348 the transition from early neural development to late neuronal differentiation in drosophila
1349 melanogaster. *PLoS ONE* 9: e97703. doi: [10.1371/journal.pone.0097703](https://doi.org/10.1371/journal.pone.0097703).
- 1350 [28] Mody M, Cao Y, Cui Z, Tay KY, Shyong A, et al. (2001) Genome-wide gene expression
1351 profiles of the developing mouse hippocampus. *Proceedings of the National Academy of*
1352 *Sciences* 98: 8862–8867. doi: [10.1073/pnas.141244998](https://doi.org/10.1073/pnas.141244998).
- 1353 [29] Suzuki R, Shimodaira H (2006) Pvcust: an r package for assessing the uncertainty in
1354 hierarchical clustering. *Bioinformatics* 22: 1540–1542. doi: [10.1093/bioinformatics/btl117](https://doi.org/10.1093/bioinformatics/btl117).
- 1355 [30] Fraser P, Bickmore W (2007) Nuclear organization of the genome and the potential for gene
1356 regulation. *Nature* 447: 413–417. doi: [10.1038/nature05916](https://doi.org/10.1038/nature05916).
- 1357 [31] Haeckel E (1874) Die gastraea-theorie, die phylogenetische classification des thierreichs und
1358 die homologie der keimblätter. *Jenaische Zeitschrift für Naturwissenschaft* 8: 1–55.

- 1359 [32] Hadzi J (1963) The evolution of the Metazoa. Macmillan.
- 1360 [33] Metschnikoff E (1886) Embryologische Studien an Medusen: ein Beitrag zur Genealogie der
1361 primitiv-Organ. A. Hölder.
- 1362 [34] Kirk DL (2005) A twelve-step program for evolving multicellularity and a division of labor.
1363 *Bioessays* 27: 299–310. doi: [10.1002/bies.20197](https://doi.org/10.1002/bies.20197).
- 1364 [35] Nielsen C (2008) Six major steps in animal evolution: are we derived sponge larvae?
1365 *Evolution & Development* 10: 241–257. doi: [10.1111/j.1525-142x.2008.00231.x](https://doi.org/10.1111/j.1525-142x.2008.00231.x).
- 1366 [36] Willensdorfer M (2009) On the evolution of differentiated multicellularity. *Evolution* 63:
1367 306–23. doi: [10.1111/j.1558-5646.2008.00541.x](https://doi.org/10.1111/j.1558-5646.2008.00541.x).
- 1368 [37] Mikhailov KV, Konstantinova AV, Nikitin MA, Troshin PV, Rusin LY, et al. (2009) The
1369 origin of metazoa: a transition from temporal to spatial cell differentiation. *Bioessays* 31:
1370 758–68. doi: [10.1002/bies.200800214](https://doi.org/10.1002/bies.200800214).
- 1371 [38] Gavrillets S (2010) Rapid transition towards the division of labor via evolution of
1372 developmental plasticity. *PLoS Computational Biology* 6: e1000805. doi:
1373 [10.1371/journal.pcbi.1000805](https://doi.org/10.1371/journal.pcbi.1000805).
- 1374 [39] Levin TC, Greaney AJ, Wetzel L, King N (2014) The rosetteless gene controls development
1375 in the choanoflagellate *S. rosetta*. *eLife* 3. doi: [10.7554/elife.04070](https://doi.org/10.7554/elife.04070).
- 1376 [40] Turing AM (1952) The chemical basis of morphogenesis. *Philosophical Transactions of the*
1377 *Royal Society of London B: Biological Sciences* 237: 37–72.
- 1378 [41] Tompkins N, Li N, Girabawe C, Heymann M, Ermentrout GB, et al. (2014) Testing Turing's
1379 theory of morphogenesis in chemical cells. *Proceedings of the National Academy of*
1380 *Sciences* 111: 4397–4402.
- 1381 [42] Kupiec JJ (1997) A darwinian theory for the origin of cellular differentiation. *Molecular and*
1382 *General Genetics* MGG 255: 201–208. doi: [10.1007/s004380050490](https://doi.org/10.1007/s004380050490).
- 1383 [43] Paldi A (2012) What makes the cell differentiate? *Prog Biophys Mol Biol* 110: 41–3. doi:
1384 [10.1016/j.pbiomolbio.2012.04.003](https://doi.org/10.1016/j.pbiomolbio.2012.04.003).
- 1385 [44] Kim J (1999) Making sense of emergence. *Philosophical Studies* 95: 3–36. doi:
1386 [10.1023/a:1004563122154](https://doi.org/10.1023/a:1004563122154).
- 1387 [45] Kim J (2006) Emergence: Core ideas and issues. *Synthese* 151: 547–559. doi:
1388 [10.1007/s11229-006-9025-0](https://doi.org/10.1007/s11229-006-9025-0).
- 1389 [46] Deacon TW (2012) *Incomplete nature: How mind emerged from matter*. New York: W.W.
1390 Norton & Co., 1st edition.
- 1391 [47] Chen L, Xiao S, Pang K, Zhou C, Yuan X (2014) Cell differentiation and germ-soma
1392 separation in ediacaran animal embryo-like fossils. *Nature* doi: [10.1038/nature13766](https://doi.org/10.1038/nature13766).
- 1393 [48] Meyerowitz EM (2002) Plants compared to animals: The broadest comparative study of
1394 development. *Science* 295: 1482–1485. doi: [10.1126/science.1066609](https://doi.org/10.1126/science.1066609).

- 1395 [49] Donoghue PCJ, Antcliffe JB (2010) Early life: Origins of multicellularity. *Nature* 466: 41–42.
1396 [doi: 10.1038/466041a](https://doi.org/10.1038/466041a).
- 1397 [50] van Nimwegen E (2003) Scaling laws in the functional content of genomes. *Trends in*
1398 *Genetics* 19: 479–484. [doi: 10.1016/s0168-9525\(03\)00203-8](https://doi.org/10.1016/s0168-9525(03)00203-8).
- 1399 [51] Wilson D, Charoensawan V, Kummerfeld SK, Teichmann SA (2007) DBD–taxonomically
1400 broad transcription factor predictions: new content and functionality. *Nucleic Acids*
1401 *Research* 36: D88–D92. [doi: 10.1093/nar/gkm964](https://doi.org/10.1093/nar/gkm964).
- 1402 [52] Young HE, Black AC (2003) Adult stem cells. *Anat Rec* 276A: 75–102. [doi:](https://doi.org/10.1002/ar.a.10134)
1403 [10.1002/ar.a.10134](https://doi.org/10.1002/ar.a.10134).
- 1404 [53] Cai S, Fu X, Sheng Z (2007) Dedifferentiation: A new approach in stem cell research.
1405 *BioScience* 57: 655. [doi: 10.1641/b570805](https://doi.org/10.1641/b570805).
- 1406 [54] Donà E, Barry JD, Valentin G, Quirin C, Khmelinskii A, et al. (2013) Directional tissue
1407 migration through a self-generated chemokine gradient. *Nature* 503: 285–9. [doi:](https://doi.org/10.1038/nature12635)
1408 [10.1038/nature12635](https://doi.org/10.1038/nature12635).
- 1409 [55] Venkiteswaran G, Lewellis SW, Wang J, Reynolds E, Nicholson C, et al. (2013) Generation
1410 and dynamics of an endogenous, self-generated signaling gradient across a migrating tissue.
1411 *Cell* 155: 674–687. [doi: 10.1016/j.cell.2013.09.046](https://doi.org/10.1016/j.cell.2013.09.046).
- 1412 [56] Kauffman S, Clayton P (2006) On emergence, agency, and organization. *Biology &*
1413 *Philosophy* 21: 501–521. [doi: 10.1007/s10539-005-9003-9](https://doi.org/10.1007/s10539-005-9003-9).
- 1414 [57] Roy S, Morse D (2012) A full suite of histone and histone modifying genes are transcribed in
1415 the dinoflagellate *Lingulodinium*. *PLoS One* 7: e34340. [doi: 10.1371/journal.pone.0034340](https://doi.org/10.1371/journal.pone.0034340).
- 1416 [58] Meletis K, Barnabé-Heider F, Carlén M, Evergren E, Tomilin N, et al. (2008) Spinal cord
1417 injury reveals multilineage differentiation of ependymal cells. *Plos Biol* 6: e182. [doi:](https://doi.org/10.1371/journal.pbio.0060182)
1418 [10.1371/journal.pbio.0060182](https://doi.org/10.1371/journal.pbio.0060182).
- 1419 [59] Sømme L (1982) Supercooling and winter survival in terrestrial arthropods. *Comparative*
1420 *Biochemistry and Physiology Part A: Physiology* 73: 519–543. [doi:](https://doi.org/10.1016/0300-9629(82)90260-2)
1421 [10.1016/0300-9629\(82\)90260-2](https://doi.org/10.1016/0300-9629(82)90260-2).
- 1422 [60] Murphy WJ, Collier GE (1997) A molecular phylogeny for aplocheiloid fishes
1423 (atherinomorpha, cyprinodontiformes): the role of vicariance and the origins of annualism.
1424 *Molecular Biology and Evolution* 14: 790–799.
- 1425 [61] Niethammer P, Grabher C, Look AT, Mitchison TJ (2009) A tissue-scale gradient of
1426 hydrogen peroxide mediates rapid wound detection in zebrafish. *Nature* 459: 996–999. [doi:](https://doi.org/10.1038/nature08119)
1427 [10.1038/nature08119](https://doi.org/10.1038/nature08119).
- 1428 [62] Unsworth BR, Lelkes PI (1998) Growing tissues in microgravity. *Nat Med* 4: 901–907. [doi:](https://doi.org/10.1038/nm0898-901)
1429 [10.1038/nm0898-901](https://doi.org/10.1038/nm0898-901).
- 1430 [63] Correll MJ, Pyle TP, Millar KDL, Sun Y, Yao J, et al. (2013) Transcriptome analyses of
1431 *Arabidopsis thaliana* seedlings grown in space: implications for gravity-responsive genes.
1432 *Planta* 238: 519–533. [doi: 10.1007/s00425-013-1909-x](https://doi.org/10.1007/s00425-013-1909-x).

- 1433 [64] Hammond T, Lewis F, Goodwin T, Linnehan R, Wolf D, et al. (1999) Gene expression in
1434 space. *Nature Medicine* 5: 359–359. doi: [10.1038/7331](https://doi.org/10.1038/7331).
- 1435 [65] Crawford-Young SJ (2006) Effects of microgravity on cell cytoskeleton and embryogenesis.
1436 *The International Journal of Developmental Biology* 50: 183–191. doi: [10.1387/ijdb.052077sc](https://doi.org/10.1387/ijdb.052077sc).
- 1437 [66] Ingber D (1999) How cells (might) sense microgravity. *The FASEB Journal* 13: S3–S15.
- 1438 [67] Pojman JA, Bessonov N, Volpert V, Paley MS (2007) Miscible fluids in microgravity (MFMG):
1439 A zero-upmass investigation on the international space station. *Microgravity Sci Technol* 19:
1440 33–41. doi: [10.1007/bf02870987](https://doi.org/10.1007/bf02870987).
- 1441 [68] Rajjou L, Duval M, Gallardo K, Catusse J, Bally J, et al. (2012) Seed germination and vigor.
1442 *Annu Rev Plant Biol* 63: 507–533. doi: [10.1146/annurev-arplant-042811-105550](https://doi.org/10.1146/annurev-arplant-042811-105550).
- 1443 [69] Finch-Savage WE, Leubner-Metzger G (2006) Seed dormancy and the control of
1444 germination. *New Phytologist* 171: 501–523. doi: [10.1111/j.1469-8137.2006.01787.x](https://doi.org/10.1111/j.1469-8137.2006.01787.x).
- 1445 [70] Smet ID, Beeckman T (2011) Asymmetric cell division in land plants and algae: the driving
1446 force for differentiation. *Nature Reviews Molecular Cell Biology* 12: 177–188. doi:
1447 [10.1038/nrm3064](https://doi.org/10.1038/nrm3064).
- 1448 [71] Greenbaum D, Colangelo C, Williams K, Gerstein M (2003) Comparing protein abundance
1449 and mrna expression levels on a genomic scale. *Genome Biol* 4: 117.
- 1450 [72] Ning K, Fermin D, Nesvizhskii AI (2012) Comparative analysis of different label-free mass
1451 spectrometry based protein abundance estimates and their correlation with RNA-seq gene
1452 expression data. *J Proteome Res* 11: 2261–2271. doi: [10.1021/pr201052x](https://doi.org/10.1021/pr201052x).
- 1453 [73] Varela FG, Maturana HR, Uribe R (1974) Autopoiesis: the organization of living systems, its
1454 characterization and a model. *Biosystems* 5: 187–196.
- 1455 [74] Celniker SE, Dillon LAL, Gerstein MB, Gunsalus KC, Henikoff S, et al. (2009) Unlocking the
1456 secrets of the genome. *Nature* 459: 927–930. doi: [10.1038/459927a](https://doi.org/10.1038/459927a).
- 1457 [75] Ram O, Goren A, Amit I, Shores N, Yosef N, et al. (2011) Combinatorial patterning of
1458 chromatin regulators uncovered by genome-wide location analysis in human cells. *Cell* 147:
1459 1628–1639. doi: [10.1016/j.cell.2011.09.057](https://doi.org/10.1016/j.cell.2011.09.057).
- 1460 [76] Nègre N, Brown CD, Ma L, Bristow CA, Miller SW, et al. (2011) A cis-regulatory map of the
1461 *Drosophila* genome. *Nature* 471: 527–531. doi: [10.1038/nature09990](https://doi.org/10.1038/nature09990).
- 1462 [77] Dunham I, Kundaje A, Aldred SF, Collins PJ, Davis CA, et al. (2012) An integrated
1463 encyclopedia of DNA elements in the human genome. *Nature* 489: 57–74. doi:
1464 [10.1038/nature11247](https://doi.org/10.1038/nature11247).
- 1465 [78] Xiao S, Xie D, Cao X, Yu P, Xing X, et al. (2012) Comparative epigenomic annotation of
1466 regulatory DNA. *Cell* 149: 1381–1392. doi: [10.1016/j.cell.2012.04.029](https://doi.org/10.1016/j.cell.2012.04.029).
- 1467 [79] Djebali S, Davis CA, Merkel A, Dobin A, Lassmann T, et al. (2012) Landscape of
1468 transcription in human cells. *Nature* 489: 101–108. doi: [10.1038/nature11233](https://doi.org/10.1038/nature11233).

- 1469 [80] Stamatoyannopoulos JA, Snyder M, Hardison R, Ren B, Gingeras T, et al. (2012) An
1470 encyclopedia of mouse DNA elements (mouse ENCODE). *Genome Biol* 13: 418. doi:
1471 [10.1186/gb-2012-13-8-418](https://doi.org/10.1186/gb-2012-13-8-418).
- 1472 [81] Trapnell C, Williams BA, Pertea G, Mortazavi A, Kwan G, et al. (2010) Transcript assembly
1473 and quantification by RNA-seq reveals unannotated transcripts and isoform switching
1474 during cell differentiation. *Nat Biotechnol* 28: 511–515. doi: [10.1038/nbt.1621](https://doi.org/10.1038/nbt.1621).
- 1475 [82] Fisher RA (1915) Frequency distribution of the values of the correlation coefficient in
1476 samples from an indefinitely large population. *Biometrika* : 507–521.
- 1477 [83] Benjamini Y, Yekutieli D (2001) The control of the false discovery rate in multiple testing
1478 under dependency. *Annals of statistics* : 1165–1188.
- 1479 [84] Saraçlı S, Doğan N, Doğan I (2013) Comparison of hierarchical cluster analysis methods by
1480 cophenetic correlation. *Journal of Inequalities and Applications* 2013: 203. doi:
1481 [10.1186/1029-242x-2013-203](https://doi.org/10.1186/1029-242x-2013-203).
- 1482 [85] R Core Team (2014) R: A Language and Environment for Statistical Computing. R
1483 Foundation for Statistical Computing, Vienna, Austria. URL <http://www.R-project.org/>.
- 1484 [86] Wagner GP, Kin K, Lynch VJ (2012) Measurement of mRNA abundance using RNA-seq
1485 data: RPKM measure is inconsistent among samples. *Theory Biosci* 131: 281–285. doi:
1486 [10.1007/s12064-012-0162-3](https://doi.org/10.1007/s12064-012-0162-3).
- 1487 [87] Altun Z, Hall D (2002). WormAtlas. URL <http://www.wormatlas.org/>.

1488 **Appendix**

1489 **Estimation of a lower bound for the necessary cell-fate information**
 1490 **capacity in the hermaphrodite *Caenorhabditis elegans* ontogeny**

Count	N ^o
Cells generated	1,090
Deaths in the process	131
Final cells	959
Cell types developed	19

1491 (Data source: WormAtlas website [87])

	Estimated as	N ^o (approx.)
Total divisions	$2^{\log_2(\text{cells_generated}+1)} - 1$	2,179
Cell-fate divisions	$2^{\log_2(\text{cell_types}+1)} - 1$	37
Non-cell-fate divisions	$\text{total_divisions} - (\text{cell_fate_divisions} + \text{deaths})$	2,011

	Estimated as	p	$-p \log_2 p$
Cell death	$\text{deaths} / \text{total_divisions}$	0.060	0.244
1492 Non-cell-fate division	$\text{non_cell_fate_divisions} / \text{total_divisions}$	0.923	0.107
Cell-fate division	$\text{cell_fate_divisions} / \text{total_divisions}$	0.017	0.1
Uncertainty per division (Sum)			0.451

	Estimated as	(bit)
1493 Uncertainty to resolve (total)	$\text{uncertainty_per_division} \times \text{total_divisions}$	983

1494 Note: germ line cells were excluded from the analysis.

1495 **Supplementary Information**

1496 ***Homo sapiens* source data of ChIP-seq on histone H3 modifications**
 1497 **(BAM/BAI files) [75]**

1498 For downloading, the URL must be constructed by adding the following prefix to each file listed:

1499

1500 <ftp://hgdownload.cse.ucsc.edu/goldenPath/hg19/encodeDCC/wgEncodeBroadHistone/>

Cell type	Antibody	GEO Accession	File URL suffix
GM12878	H3K27ac	GSM733771	wgEncodeBroadHistoneGm12878H3k27acStdA1nRep1.bam.bai
GM12878	H3K27ac	GSM733771	wgEncodeBroadHistoneGm12878H3k27acStdA1nRep1.bam
GM12878	H3K27ac	GSM733771	wgEncodeBroadHistoneGm12878H3k27acStdA1nRep2.bam.bai
GM12878	H3K27ac	GSM733771	wgEncodeBroadHistoneGm12878H3k27acStdA1nRep2.bam
GM12878	H3K27me3	GSM733758	wgEncodeBroadHistoneGm12878H3k27me3StdA1nRep1.bam.bai
GM12878	H3K27me3	GSM733758	wgEncodeBroadHistoneGm12878H3k27me3StdA1nRep1.bam
GM12878	H3K27me3	GSM733758	wgEncodeBroadHistoneGm12878H3k27me3StdA1nRep2.bam.bai
GM12878	H3K27me3	GSM733758	wgEncodeBroadHistoneGm12878H3k27me3StdA1nRep2.bam
GM12878	H3K27me3	GSM733758	wgEncodeBroadHistoneGm12878H3k27me3StdA1nRep3V2.bam.bai
GM12878	H3K27me3	GSM733758	wgEncodeBroadHistoneGm12878H3k27me3StdA1nRep3V2.bam
GM12878	H3K36me3	GSM733679	wgEncodeBroadHistoneGm12878H3k36me3StdA1nRep1.bam.bai
GM12878	H3K36me3	GSM733679	wgEncodeBroadHistoneGm12878H3k36me3StdA1nRep1.bam
GM12878	H3K36me3	GSM733679	wgEncodeBroadHistoneGm12878H3k36me3StdA1nRep2.bam.bai
GM12878	H3K36me3	GSM733679	wgEncodeBroadHistoneGm12878H3k36me3StdA1nRep2.bam
GM12878	H3K4me1	GSM733772	wgEncodeBroadHistoneGm12878H3k4me1StdA1nRep2.bam.bai
GM12878	H3K4me1	GSM733772	wgEncodeBroadHistoneGm12878H3k4me1StdA1nRep2.bam
GM12878	H3K4me1	GSM733772	wgEncodeBroadHistoneGm12878H3k04me1StdA1nRep1V2.bam.bai
GM12878	H3K4me1	GSM733772	wgEncodeBroadHistoneGm12878H3k04me1StdA1nRep1V2.bam
GM12878	H3K4me2	GSM733769	wgEncodeBroadHistoneGm12878H3k4me2StdA1nRep1.bam.bai
GM12878	H3K4me2	GSM733769	wgEncodeBroadHistoneGm12878H3k4me2StdA1nRep1.bam
GM12878	H3K4me2	GSM733769	wgEncodeBroadHistoneGm12878H3k4me2StdA1nRep2.bam.bai
GM12878	H3K4me2	GSM733769	wgEncodeBroadHistoneGm12878H3k4me2StdA1nRep2.bam
GM12878	H3K4me3	GSM733708	wgEncodeBroadHistoneGm12878H3k04me3StdA1nRep2V2.bam.bai
GM12878	H3K4me3	GSM733708	wgEncodeBroadHistoneGm12878H3k04me3StdA1nRep2V2.bam
GM12878	H3K4me3	GSM733708	wgEncodeBroadHistoneGm12878H3k4me3StdA1nRep1.bam.bai
GM12878	H3K4me3	GSM733708	wgEncodeBroadHistoneGm12878H3k4me3StdA1nRep1.bam
GM12878	H3K79me2	GSM733736	wgEncodeBroadHistoneGm12878H3k79me2StdA1nRep1.bam.bai
GM12878	H3K79me2	GSM733736	wgEncodeBroadHistoneGm12878H3k79me2StdA1nRep1.bam
GM12878	H3K79me2	GSM733736	wgEncodeBroadHistoneGm12878H3k79me2StdA1nRep2.bam.bai
GM12878	H3K79me2	GSM733736	wgEncodeBroadHistoneGm12878H3k79me2StdA1nRep2.bam
GM12878	H3K9ac	GSM733677	wgEncodeBroadHistoneGm12878H3k9acStdA1nRep1.bam.bai
GM12878	H3K9ac	GSM733677	wgEncodeBroadHistoneGm12878H3k9acStdA1nRep1.bam
GM12878	H3K9ac	GSM733677	wgEncodeBroadHistoneGm12878H3k9acStdA1nRep2.bam.bai
GM12878	H3K9ac	GSM733677	wgEncodeBroadHistoneGm12878H3k9acStdA1nRep2.bam
GM12878	H3K9me3	GSM733664	wgEncodeBroadHistoneGm12878H3k9me3StdA1nRep1.bam.bai
GM12878	H3K9me3	GSM733664	wgEncodeBroadHistoneGm12878H3k9me3StdA1nRep1.bam
GM12878	H3K9me3	GSM733664	wgEncodeBroadHistoneGm12878H3k9me3StdA1nRep2.bam.bai
GM12878	H3K9me3	GSM733664	wgEncodeBroadHistoneGm12878H3k9me3StdA1nRep2.bam
GM12878	H3K9me3	GSM733664	wgEncodeBroadHistoneGm12878H3k9me3StdA1nRep3.bam.bai
GM12878	H3K9me3	GSM733664	wgEncodeBroadHistoneGm12878H3k9me3StdA1nRep3.bam

Continued on next page

Continued from previous page

Cell type	Antibody	GEO Accession	File URL suffix
GM12878	Input	GSM733742	wgEncodeBroadHistoneGm12878ControlStdA1nRep1.bam.bai
GM12878	Input	GSM733742	wgEncodeBroadHistoneGm12878ControlStdA1nRep1.bam
GM12878	Input	GSM733742	wgEncodeBroadHistoneGm12878ControlStdA1nRep2.bam.bai
GM12878	Input	GSM733742	wgEncodeBroadHistoneGm12878ControlStdA1nRep2.bam
H1-hESC	H3K27ac	GSM733718	wgEncodeBroadHistoneH1hescH3k27acStdA1nRep1.bam.bai
H1-hESC	H3K27ac	GSM733718	wgEncodeBroadHistoneH1hescH3k27acStdA1nRep1.bam
H1-hESC	H3K27ac	GSM733718	wgEncodeBroadHistoneH1hescH3k27acStdA1nRep2.bam.bai
H1-hESC	H3K27ac	GSM733718	wgEncodeBroadHistoneH1hescH3k27acStdA1nRep2.bam
H1-hESC	H3K27me3	GSM733748	wgEncodeBroadHistoneH1hescH3k27me3StdA1nRep1.bam.bai
H1-hESC	H3K27me3	GSM733748	wgEncodeBroadHistoneH1hescH3k27me3StdA1nRep1.bam
H1-hESC	H3K27me3	GSM733748	wgEncodeBroadHistoneH1hescH3k27me3StdA1nRep2.bam.bai
H1-hESC	H3K27me3	GSM733748	wgEncodeBroadHistoneH1hescH3k27me3StdA1nRep2.bam
H1-hESC	H3K36me3	GSM733725	wgEncodeBroadHistoneH1hescH3k36me3StdA1nRep1.bam.bai
H1-hESC	H3K36me3	GSM733725	wgEncodeBroadHistoneH1hescH3k36me3StdA1nRep1.bam
H1-hESC	H3K36me3	GSM733725	wgEncodeBroadHistoneH1hescH3k36me3StdA1nRep2.bam.bai
H1-hESC	H3K36me3	GSM733725	wgEncodeBroadHistoneH1hescH3k36me3StdA1nRep2.bam
H1-hESC	H3K4me1	GSM733782	wgEncodeBroadHistoneH1hescH3k4me1StdA1nRep1.bam.bai
H1-hESC	H3K4me1	GSM733782	wgEncodeBroadHistoneH1hescH3k4me1StdA1nRep1.bam
H1-hESC	H3K4me1	GSM733782	wgEncodeBroadHistoneH1hescH3k4me1StdA1nRep2.bam.bai
H1-hESC	H3K4me1	GSM733782	wgEncodeBroadHistoneH1hescH3k4me1StdA1nRep2.bam
H1-hESC	H3K4me2	GSM733670	wgEncodeBroadHistoneH1hescH3k4me2StdA1nRep1.bam.bai
H1-hESC	H3K4me2	GSM733670	wgEncodeBroadHistoneH1hescH3k4me2StdA1nRep1.bam
H1-hESC	H3K4me2	GSM733670	wgEncodeBroadHistoneH1hescH3k4me2StdA1nRep2.bam.bai
H1-hESC	H3K4me2	GSM733670	wgEncodeBroadHistoneH1hescH3k4me2StdA1nRep2.bam
H1-hESC	H3K4me3	GSM733657	wgEncodeBroadHistoneH1hescH3k4me3StdA1nRep1.bam.bai
H1-hESC	H3K4me3	GSM733657	wgEncodeBroadHistoneH1hescH3k4me3StdA1nRep1.bam
H1-hESC	H3K4me3	GSM733657	wgEncodeBroadHistoneH1hescH3k4me3StdA1nRep2.bam.bai
H1-hESC	H3K4me3	GSM733657	wgEncodeBroadHistoneH1hescH3k4me3StdA1nRep2.bam
H1-hESC	H3K79me2	GSM1003547	wgEncodeBroadHistoneH1hescH3k79me2StdA1nRep1.bam.bai
H1-hESC	H3K79me2	GSM1003547	wgEncodeBroadHistoneH1hescH3k79me2StdA1nRep1.bam
H1-hESC	H3K79me2	GSM1003547	wgEncodeBroadHistoneH1hescH3k79me2StdA1nRep2.bam.bai
H1-hESC	H3K79me2	GSM1003547	wgEncodeBroadHistoneH1hescH3k79me2StdA1nRep2.bam
H1-hESC	H3K9ac	GSM733773	wgEncodeBroadHistoneH1hescH3k9acStdA1nRep1.bam.bai
H1-hESC	H3K9ac	GSM733773	wgEncodeBroadHistoneH1hescH3k9acStdA1nRep1.bam
H1-hESC	H3K9ac	GSM733773	wgEncodeBroadHistoneH1hescH3k9acStdA1nRep2.bam.bai
H1-hESC	H3K9ac	GSM733773	wgEncodeBroadHistoneH1hescH3k9acStdA1nRep2.bam
H1-hESC	H3K9me3	GSM1003585	wgEncodeBroadHistoneH1hescH3k09me3StdA1nRep1.bam.bai
H1-hESC	H3K9me3	GSM1003585	wgEncodeBroadHistoneH1hescH3k09me3StdA1nRep1.bam
H1-hESC	H3K9me3	GSM1003585	wgEncodeBroadHistoneH1hescH3k09me3StdA1nRep2.bam.bai
H1-hESC	H3K9me3	GSM1003585	wgEncodeBroadHistoneH1hescH3k09me3StdA1nRep2.bam
H1-hESC	Input	GSM733770	wgEncodeBroadHistoneH1hescControlStdA1nRep1.bam.bai
H1-hESC	Input	GSM733770	wgEncodeBroadHistoneH1hescControlStdA1nRep1.bam
H1-hESC	Input	GSM733770	wgEncodeBroadHistoneH1hescControlStdA1nRep2.bam.bai
H1-hESC	Input	GSM733770	wgEncodeBroadHistoneH1hescControlStdA1nRep2.bam
HSM1	H3K27ac	GSM733755	wgEncodeBroadHistoneHsmmH3k27acStdA1nRep1.bam.bai
HSM1	H3K27ac	GSM733755	wgEncodeBroadHistoneHsmmH3k27acStdA1nRep1.bam
HSM1	H3K27ac	GSM733755	wgEncodeBroadHistoneHsmmH3k27acStdA1nRep2.bam.bai
HSM1	H3K27ac	GSM733755	wgEncodeBroadHistoneHsmmH3k27acStdA1nRep2.bam
HSM1	H3K27me3	GSM733667	wgEncodeBroadHistoneHsmmH3k27me3StdA1nRep1.bam.bai
HSM1	H3K27me3	GSM733667	wgEncodeBroadHistoneHsmmH3k27me3StdA1nRep1.bam
HSM1	H3K27me3	GSM733667	wgEncodeBroadHistoneHsmmH3k27me3StdA1nRep2.bam.bai

Continued on next page

Continued from previous page

Cell type	Antibody	GEO Accession	File URL suffix
HSMM	H3K27me3	GSM733667	wgEncodeBroadHistoneHsmmH3k27me3StdA1nRep2.bam
HSMM	H3K36me3	GSM733702	wgEncodeBroadHistoneHsmmH3k36me3StdA1nRep1.bam.bai
HSMM	H3K36me3	GSM733702	wgEncodeBroadHistoneHsmmH3k36me3StdA1nRep1.bam
HSMM	H3K36me3	GSM733702	wgEncodeBroadHistoneHsmmH3k36me3StdA1nRep2.bam.bai
HSMM	H3K36me3	GSM733702	wgEncodeBroadHistoneHsmmH3k36me3StdA1nRep2.bam
HSMM	H3K4me1	GSM733761	wgEncodeBroadHistoneHsmmH3k4me1StdA1nRep1.bam.bai
HSMM	H3K4me1	GSM733761	wgEncodeBroadHistoneHsmmH3k4me1StdA1nRep1.bam
HSMM	H3K4me1	GSM733761	wgEncodeBroadHistoneHsmmH3k4me1StdA1nRep2.bam.bai
HSMM	H3K4me1	GSM733761	wgEncodeBroadHistoneHsmmH3k4me1StdA1nRep2.bam
HSMM	H3K4me2	GSM733768	wgEncodeBroadHistoneHsmmH3k4me2StdA1nRep1.bam.bai
HSMM	H3K4me2	GSM733768	wgEncodeBroadHistoneHsmmH3k4me2StdA1nRep1.bam
HSMM	H3K4me2	GSM733768	wgEncodeBroadHistoneHsmmH3k4me2StdA1nRep2.bam.bai
HSMM	H3K4me2	GSM733768	wgEncodeBroadHistoneHsmmH3k4me2StdA1nRep2.bam
HSMM	H3K4me3	GSM733637	wgEncodeBroadHistoneHsmmH3k4me3StdA1nRep1.bam.bai
HSMM	H3K4me3	GSM733637	wgEncodeBroadHistoneHsmmH3k4me3StdA1nRep1.bam
HSMM	H3K4me3	GSM733637	wgEncodeBroadHistoneHsmmH3k4me3StdA1nRep2.bam.bai
HSMM	H3K4me3	GSM733637	wgEncodeBroadHistoneHsmmH3k4me3StdA1nRep2.bam
HSMM	H3K79me2	GSM733741	wgEncodeBroadHistoneHsmmH3k79me2StdA1nRep1.bam.bai
HSMM	H3K79me2	GSM733741	wgEncodeBroadHistoneHsmmH3k79me2StdA1nRep1.bam
HSMM	H3K79me2	GSM733741	wgEncodeBroadHistoneHsmmH3k79me2StdA1nRep2.bam.bai
HSMM	H3K79me2	GSM733741	wgEncodeBroadHistoneHsmmH3k79me2StdA1nRep2.bam
HSMM	H3K9ac	GSM733775	wgEncodeBroadHistoneHsmmH3k9acStdA1nRep1.bam.bai
HSMM	H3K9ac	GSM733775	wgEncodeBroadHistoneHsmmH3k9acStdA1nRep1.bam
HSMM	H3K9ac	GSM733775	wgEncodeBroadHistoneHsmmH3k9acStdA1nRep2.bam.bai
HSMM	H3K9ac	GSM733775	wgEncodeBroadHistoneHsmmH3k9acStdA1nRep2.bam
HSMM	H3K9me3	GSM733730	wgEncodeBroadHistoneHsmmH3k9me3StdA1nRep1.bam.bai
HSMM	H3K9me3	GSM733730	wgEncodeBroadHistoneHsmmH3k9me3StdA1nRep1.bam
HSMM	H3K9me3	GSM733730	wgEncodeBroadHistoneHsmmH3k9me3StdA1nRep2.bam.bai
HSMM	H3K9me3	GSM733730	wgEncodeBroadHistoneHsmmH3k9me3StdA1nRep2.bam
HSMM	Input	GSM733663	wgEncodeBroadHistoneHsmmControlStdA1nRep1.bam.bai
HSMM	Input	GSM733663	wgEncodeBroadHistoneHsmmControlStdA1nRep1.bam
HSMM	Input	GSM733663	wgEncodeBroadHistoneHsmmControlStdA1nRep2.bam.bai
HSMM	Input	GSM733663	wgEncodeBroadHistoneHsmmControlStdA1nRep2.bam
HUVEC	H3K27ac	GSM733691	wgEncodeBroadHistoneHuvecH3k27acStdA1nRep1.bam.bai
HUVEC	H3K27ac	GSM733691	wgEncodeBroadHistoneHuvecH3k27acStdA1nRep1.bam
HUVEC	H3K27ac	GSM733691	wgEncodeBroadHistoneHuvecH3k27acStdA1nRep2.bam.bai
HUVEC	H3K27ac	GSM733691	wgEncodeBroadHistoneHuvecH3k27acStdA1nRep2.bam
HUVEC	H3K27ac	GSM733691	wgEncodeBroadHistoneHuvecH3k27acStdA1nRep3.bam.bai
HUVEC	H3K27ac	GSM733691	wgEncodeBroadHistoneHuvecH3k27acStdA1nRep3.bam
HUVEC	H3K27me3	GSM733688	wgEncodeBroadHistoneHuvecH3k27me3StdA1nRep1.bam.bai
HUVEC	H3K27me3	GSM733688	wgEncodeBroadHistoneHuvecH3k27me3StdA1nRep1.bam
HUVEC	H3K27me3	GSM733688	wgEncodeBroadHistoneHuvecH3k27me3StdA1nRep2.bam.bai
HUVEC	H3K27me3	GSM733688	wgEncodeBroadHistoneHuvecH3k27me3StdA1nRep2.bam
HUVEC	H3K36me3	GSM733757	wgEncodeBroadHistoneHuvecH3k36me3StdA1nRep1.bam.bai
HUVEC	H3K36me3	GSM733757	wgEncodeBroadHistoneHuvecH3k36me3StdA1nRep1.bam
HUVEC	H3K36me3	GSM733757	wgEncodeBroadHistoneHuvecH3k36me3StdA1nRep2.bam.bai
HUVEC	H3K36me3	GSM733757	wgEncodeBroadHistoneHuvecH3k36me3StdA1nRep2.bam
HUVEC	H3K36me3	GSM733757	wgEncodeBroadHistoneHuvecH3k36me3StdA1nRep3.bam.bai
HUVEC	H3K36me3	GSM733757	wgEncodeBroadHistoneHuvecH3k36me3StdA1nRep3.bam
HUVEC	H3K4me1	GSM733690	wgEncodeBroadHistoneHuvecH3k4me1StdA1nRep1.bam.bai
HUVEC	H3K4me1	GSM733690	wgEncodeBroadHistoneHuvecH3k4me1StdA1nRep1.bam

Continued on next page

Continued from previous page

Cell type	Antibody	GEO Accession	File URL suffix
HUVEC	H3K4me1	GSM733690	wgEncodeBroadHistoneHuvecH3k4me1StdA1nRep2.bam.bai
HUVEC	H3K4me1	GSM733690	wgEncodeBroadHistoneHuvecH3k4me1StdA1nRep2.bam
HUVEC	H3K4me1	GSM733690	wgEncodeBroadHistoneHuvecH3k4me1StdA1nRep3.bam.bai
HUVEC	H3K4me1	GSM733690	wgEncodeBroadHistoneHuvecH3k4me1StdA1nRep3.bam
HUVEC	H3K4me2	GSM733683	wgEncodeBroadHistoneHuvecH3k4me2StdA1nRep1.bam.bai
HUVEC	H3K4me2	GSM733683	wgEncodeBroadHistoneHuvecH3k4me2StdA1nRep1.bam
HUVEC	H3K4me2	GSM733683	wgEncodeBroadHistoneHuvecH3k4me2StdA1nRep2.bam.bai
HUVEC	H3K4me2	GSM733683	wgEncodeBroadHistoneHuvecH3k4me2StdA1nRep2.bam
HUVEC	H3K4me3	GSM733673	wgEncodeBroadHistoneHuvecH3k4me3StdA1nRep1.bam.bai
HUVEC	H3K4me3	GSM733673	wgEncodeBroadHistoneHuvecH3k4me3StdA1nRep1.bam
HUVEC	H3K4me3	GSM733673	wgEncodeBroadHistoneHuvecH3k4me3StdA1nRep2.bam.bai
HUVEC	H3K4me3	GSM733673	wgEncodeBroadHistoneHuvecH3k4me3StdA1nRep2.bam
HUVEC	H3K4me3	GSM733673	wgEncodeBroadHistoneHuvecH3k4me3StdA1nRep3.bam.bai
HUVEC	H3K4me3	GSM733673	wgEncodeBroadHistoneHuvecH3k4me3StdA1nRep3.bam
HUVEC	H3K79me2	GSM1003555	wgEncodeBroadHistoneHuvecH3k79me2A1nRep1.bam.bai
HUVEC	H3K79me2	GSM1003555	wgEncodeBroadHistoneHuvecH3k79me2A1nRep1.bam
HUVEC	H3K79me2	GSM1003555	wgEncodeBroadHistoneHuvecH3k79me2A1nRep2.bam.bai
HUVEC	H3K79me2	GSM1003555	wgEncodeBroadHistoneHuvecH3k79me2A1nRep2.bam
HUVEC	H3K9ac	GSM733735	wgEncodeBroadHistoneHuvecH3k9acStdA1nRep1.bam.bai
HUVEC	H3K9ac	GSM733735	wgEncodeBroadHistoneHuvecH3k9acStdA1nRep1.bam
HUVEC	H3K9ac	GSM733735	wgEncodeBroadHistoneHuvecH3k9acStdA1nRep2.bam.bai
HUVEC	H3K9ac	GSM733735	wgEncodeBroadHistoneHuvecH3k9acStdA1nRep2.bam
HUVEC	H3K9ac	GSM733735	wgEncodeBroadHistoneHuvecH3k9acStdA1nRep3.bam.bai
HUVEC	H3K9ac	GSM733735	wgEncodeBroadHistoneHuvecH3k9acStdA1nRep3.bam
HUVEC	H3K9me3	GSM1003517	wgEncodeBroadHistoneHuvecH3k09me3A1nRep1.bam.bai
HUVEC	H3K9me3	GSM1003517	wgEncodeBroadHistoneHuvecH3k09me3A1nRep1.bam
HUVEC	H3K9me3	GSM1003517	wgEncodeBroadHistoneHuvecH3k09me3A1nRep2.bam.bai
HUVEC	H3K9me3	GSM1003517	wgEncodeBroadHistoneHuvecH3k09me3A1nRep2.bam
HUVEC	Input	GSM733715	wgEncodeBroadHistoneHuvecControlStdA1nRep1.bam.bai
HUVEC	Input	GSM733715	wgEncodeBroadHistoneHuvecControlStdA1nRep1.bam
HUVEC	Input	GSM733715	wgEncodeBroadHistoneHuvecControlStdA1nRep2.bam.bai
HUVEC	Input	GSM733715	wgEncodeBroadHistoneHuvecControlStdA1nRep2.bam
HUVEC	Input	GSM733715	wgEncodeBroadHistoneHuvecControlStdA1nRep3.bam.bai
HUVEC	Input	GSM733715	wgEncodeBroadHistoneHuvecControlStdA1nRep3.bam
NHEK	H3K27ac	GSM733674	wgEncodeBroadHistoneNhekH3k27acStdA1nRep1.bam.bai
NHEK	H3K27ac	GSM733674	wgEncodeBroadHistoneNhekH3k27acStdA1nRep1.bam
NHEK	H3K27ac	GSM733674	wgEncodeBroadHistoneNhekH3k27acStdA1nRep2.bam.bai
NHEK	H3K27ac	GSM733674	wgEncodeBroadHistoneNhekH3k27acStdA1nRep2.bam
NHEK	H3K27ac	GSM733674	wgEncodeBroadHistoneNhekH3k27acStdA1nRep3.bam.bai
NHEK	H3K27ac	GSM733674	wgEncodeBroadHistoneNhekH3k27acStdA1nRep3.bam
NHEK	H3K27me3	GSM733701	wgEncodeBroadHistoneNhekH3k27me3StdA1nRep1.bam.bai
NHEK	H3K27me3	GSM733701	wgEncodeBroadHistoneNhekH3k27me3StdA1nRep1.bam
NHEK	H3K27me3	GSM733701	wgEncodeBroadHistoneNhekH3k27me3StdA1nRep2.bam.bai
NHEK	H3K27me3	GSM733701	wgEncodeBroadHistoneNhekH3k27me3StdA1nRep2.bam
NHEK	H3K27me3	GSM733701	wgEncodeBroadHistoneNhekH3k27me3StdA1nRep3.bam.bai
NHEK	H3K27me3	GSM733701	wgEncodeBroadHistoneNhekH3k27me3StdA1nRep3.bam
NHEK	H3K36me3	GSM733726	wgEncodeBroadHistoneNhekH3k36me3StdA1nRep1.bam.bai
NHEK	H3K36me3	GSM733726	wgEncodeBroadHistoneNhekH3k36me3StdA1nRep1.bam
NHEK	H3K36me3	GSM733726	wgEncodeBroadHistoneNhekH3k36me3StdA1nRep2.bam.bai
NHEK	H3K36me3	GSM733726	wgEncodeBroadHistoneNhekH3k36me3StdA1nRep2.bam
NHEK	H3K36me3	GSM733726	wgEncodeBroadHistoneNhekH3k36me3StdA1nRep3.bam.bai
NHEK	H3K36me3	GSM733726	wgEncodeBroadHistoneNhekH3k36me3StdA1nRep3.bam

Continued on next page

Continued from previous page

Cell type	Antibody	GEO Accession	File URL suffix
NHEK	H3K36me3	GSM733726	wgEncodeBroadHistoneNhekH3k36me3StdA1nRep3.bam
NHEK	H3K4me1	GSM733698	wgEncodeBroadHistoneNhekH3k4me1StdA1nRep1.bam.bai
NHEK	H3K4me1	GSM733698	wgEncodeBroadHistoneNhekH3k4me1StdA1nRep1.bam
NHEK	H3K4me1	GSM733698	wgEncodeBroadHistoneNhekH3k4me1StdA1nRep2.bam.bai
NHEK	H3K4me1	GSM733698	wgEncodeBroadHistoneNhekH3k4me1StdA1nRep2.bam
NHEK	H3K4me1	GSM733698	wgEncodeBroadHistoneNhekH3k4me1StdA1nRep3.bam.bai
NHEK	H3K4me1	GSM733698	wgEncodeBroadHistoneNhekH3k4me1StdA1nRep3.bam
NHEK	H3K4me2	GSM733686	wgEncodeBroadHistoneNhekH3k4me2StdA1nRep1.bam.bai
NHEK	H3K4me2	GSM733686	wgEncodeBroadHistoneNhekH3k4me2StdA1nRep1.bam
NHEK	H3K4me2	GSM733686	wgEncodeBroadHistoneNhekH3k4me2StdA1nRep2.bam.bai
NHEK	H3K4me2	GSM733686	wgEncodeBroadHistoneNhekH3k4me2StdA1nRep2.bam
NHEK	H3K4me2	GSM733686	wgEncodeBroadHistoneNhekH3k4me2StdA1nRep3.bam.bai
NHEK	H3K4me2	GSM733686	wgEncodeBroadHistoneNhekH3k4me2StdA1nRep3.bam
NHEK	H3K4me3	GSM733720	wgEncodeBroadHistoneNhekH3k4me3StdA1nRep1.bam.bai
NHEK	H3K4me3	GSM733720	wgEncodeBroadHistoneNhekH3k4me3StdA1nRep1.bam
NHEK	H3K4me3	GSM733720	wgEncodeBroadHistoneNhekH3k4me3StdA1nRep2.bam.bai
NHEK	H3K4me3	GSM733720	wgEncodeBroadHistoneNhekH3k4me3StdA1nRep2.bam
NHEK	H3K4me3	GSM733720	wgEncodeBroadHistoneNhekH3k4me3StdA1nRep3.bam.bai
NHEK	H3K4me3	GSM733720	wgEncodeBroadHistoneNhekH3k4me3StdA1nRep3.bam
NHEK	H3K79me2	GSM1003527	wgEncodeBroadHistoneNhekH3k79me2A1nRep1.bam.bai
NHEK	H3K79me2	GSM1003527	wgEncodeBroadHistoneNhekH3k79me2A1nRep1.bam
NHEK	H3K79me2	GSM1003527	wgEncodeBroadHistoneNhekH3k79me2A1nRep2.bam.bai
NHEK	H3K79me2	GSM1003527	wgEncodeBroadHistoneNhekH3k79me2A1nRep2.bam
NHEK	H3K9ac	GSM733665	wgEncodeBroadHistoneNhekH3k9acStdA1nRep1.bam.bai
NHEK	H3K9ac	GSM733665	wgEncodeBroadHistoneNhekH3k9acStdA1nRep1.bam
NHEK	H3K9ac	GSM733665	wgEncodeBroadHistoneNhekH3k9acStdA1nRep2.bam.bai
NHEK	H3K9ac	GSM733665	wgEncodeBroadHistoneNhekH3k9acStdA1nRep2.bam
NHEK	H3K9ac	GSM733665	wgEncodeBroadHistoneNhekH3k9acStdA1nRep3.bam.bai
NHEK	H3K9ac	GSM733665	wgEncodeBroadHistoneNhekH3k9acStdA1nRep3.bam
NHEK	H3K9me3	GSM1003528	wgEncodeBroadHistoneNhekH3k09me3A1nRep1.bam.bai
NHEK	H3K9me3	GSM1003528	wgEncodeBroadHistoneNhekH3k09me3A1nRep1.bam
NHEK	H3K9me3	GSM1003528	wgEncodeBroadHistoneNhekH3k09me3A1nRep2.bam.bai
NHEK	H3K9me3	GSM1003528	wgEncodeBroadHistoneNhekH3k09me3A1nRep2.bam
NHEK	Input	GSM733740	wgEncodeBroadHistoneNhekControlStdA1nRep1.bam.bai
NHEK	Input	GSM733740	wgEncodeBroadHistoneNhekControlStdA1nRep1.bam
NHEK	Input	GSM733740	wgEncodeBroadHistoneNhekControlStdA1nRep2.bam.bai
NHEK	Input	GSM733740	wgEncodeBroadHistoneNhekControlStdA1nRep2.bam
NHLF	H3K27ac	GSM733646	wgEncodeBroadHistoneNhl1fH3k27acStdA1nRep1.bam.bai
NHLF	H3K27ac	GSM733646	wgEncodeBroadHistoneNhl1fH3k27acStdA1nRep1.bam
NHLF	H3K27ac	GSM733646	wgEncodeBroadHistoneNhl1fH3k27acStdA1nRep2.bam.bai
NHLF	H3K27ac	GSM733646	wgEncodeBroadHistoneNhl1fH3k27acStdA1nRep2.bam
NHLF	H3K27me3	GSM733764	wgEncodeBroadHistoneNhl1fH3k27me3StdA1nRep1.bam.bai
NHLF	H3K27me3	GSM733764	wgEncodeBroadHistoneNhl1fH3k27me3StdA1nRep1.bam
NHLF	H3K27me3	GSM733764	wgEncodeBroadHistoneNhl1fH3k27me3StdA1nRep2.bam.bai
NHLF	H3K27me3	GSM733764	wgEncodeBroadHistoneNhl1fH3k27me3StdA1nRep2.bam
NHLF	H3K36me3	GSM733699	wgEncodeBroadHistoneNhl1fH3k36me3StdA1nRep1.bam.bai
NHLF	H3K36me3	GSM733699	wgEncodeBroadHistoneNhl1fH3k36me3StdA1nRep1.bam
NHLF	H3K36me3	GSM733699	wgEncodeBroadHistoneNhl1fH3k36me3StdA1nRep2.bam.bai
NHLF	H3K36me3	GSM733699	wgEncodeBroadHistoneNhl1fH3k36me3StdA1nRep2.bam
NHLF	H3K4me1	GSM733649	wgEncodeBroadHistoneNhl1fH3k4me1StdA1nRep1.bam.bai
NHLF	H3K4me1	GSM733649	wgEncodeBroadHistoneNhl1fH3k4me1StdA1nRep1.bam

Continued on next page

Continued from previous page

Cell type	Antibody	GEO Accession	File URL suffix
NHLF	H3K4me1	GSM733649	wgEncodeBroadHistoneNhlFh3k4me1StdA1nRep2.bam.bai
NHLF	H3K4me1	GSM733649	wgEncodeBroadHistoneNhlFh3k4me1StdA1nRep2.bam
NHLF	H3K4me2	GSM733781	wgEncodeBroadHistoneNhlFh3k4me2StdA1nRep1.bam.bai
NHLF	H3K4me2	GSM733781	wgEncodeBroadHistoneNhlFh3k4me2StdA1nRep1.bam
NHLF	H3K4me2	GSM733781	wgEncodeBroadHistoneNhlFh3k4me2StdA1nRep2.bam.bai
NHLF	H3K4me2	GSM733781	wgEncodeBroadHistoneNhlFh3k4me2StdA1nRep2.bam
NHLF	H3K4me3	GSM733723	wgEncodeBroadHistoneNhlFh3k4me3StdA1nRep1.bam.bai
NHLF	H3K4me3	GSM733723	wgEncodeBroadHistoneNhlFh3k4me3StdA1nRep1.bam
NHLF	H3K4me3	GSM733723	wgEncodeBroadHistoneNhlFh3k4me3StdA1nRep2.bam.bai
NHLF	H3K4me3	GSM733723	wgEncodeBroadHistoneNhlFh3k4me3StdA1nRep2.bam
NHLF	H3K79me2	GSM1003549	wgEncodeBroadHistoneNhlFh3k79me2A1nRep1.bam.bai
NHLF	H3K79me2	GSM1003549	wgEncodeBroadHistoneNhlFh3k79me2A1nRep1.bam
NHLF	H3K79me2	GSM1003549	wgEncodeBroadHistoneNhlFh3k79me2A1nRep2.bam.bai
NHLF	H3K79me2	GSM1003549	wgEncodeBroadHistoneNhlFh3k79me2A1nRep2.bam
NHLF	H3K9ac	GSM733652	wgEncodeBroadHistoneNhlFh3k9acStdA1nRep1.bam.bai
NHLF	H3K9ac	GSM733652	wgEncodeBroadHistoneNhlFh3k9acStdA1nRep1.bam
NHLF	H3K9ac	GSM733652	wgEncodeBroadHistoneNhlFh3k9acStdA1nRep2.bam.bai
NHLF	H3K9ac	GSM733652	wgEncodeBroadHistoneNhlFh3k9acStdA1nRep2.bam
NHLF	H3K9me3	GSM1003531	wgEncodeBroadHistoneNhlFh3k09me3A1nRep1.bam.bai
NHLF	H3K9me3	GSM1003531	wgEncodeBroadHistoneNhlFh3k09me3A1nRep1.bam
NHLF	H3K9me3	GSM1003531	wgEncodeBroadHistoneNhlFh3k09me3A1nRep2.bam.bai
NHLF	H3K9me3	GSM1003531	wgEncodeBroadHistoneNhlFh3k09me3A1nRep2.bam
NHLF	Input	GSM733731	wgEncodeBroadHistoneNhlFcontrolStdA1nRep1.bam.bai
NHLF	Input	GSM733731	wgEncodeBroadHistoneNhlFcontrolStdA1nRep1.bam
NHLF	Input	GSM733731	wgEncodeBroadHistoneNhlFcontrolStdA1nRep2.bam.bai
NHLF	Input	GSM733731	wgEncodeBroadHistoneNhlFcontrolStdA1nRep2.bam

1501

1502 ***Homo sapiens* source data of RNA-seq transcript abundance in FPKM**
 1503 **(GTF files) [79]**

1504 For downloading, the URL must be constructed by adding the following prefix to each file listed:

1505

1506 <ftp://hgdownload.cse.ucsc.edu/goldenPath/hg19/encodeDCC/wgEncodeCaltechRnaSeq/>

Cell type	GEO Accession	File URL suffix
GM12878	GSM958728	wgEncodeCaltechRnaSeqGm12878R2x75I1200TSSRep1V3.gtf.gz
GM12878	GSM958728	wgEncodeCaltechRnaSeqGm12878R2x75I1200TSSRep2V3.gtf.gz
H1-hESC	GSM958733	wgEncodeCaltechRnaSeqH1hescR2x75I1200TSSRep1V3.gtf.gz
H1-hESC	GSM958733	wgEncodeCaltechRnaSeqH1hescR2x75I1200TSSRep2V3.gtf.gz
H1-hESC	GSM958733	wgEncodeCaltechRnaSeqH1hescR2x75I1200TSSRep3V3.gtf.gz
H1-hESC	GSM958733	wgEncodeCaltechRnaSeqH1hescR2x75I1200TSSRep4V3.gtf.gz
HSMM	GSM958744	wgEncodeCaltechRnaSeqHsmmR2x75I1200TSSRep1V3.gtf.gz
HSMM	GSM958744	wgEncodeCaltechRnaSeqHsmmR2x75I1200TSSRep2V3.gtf.gz
HUVEC	GSM958734	wgEncodeCaltechRnaSeqHuvecR2x75I1200TSSRep1V3.gtf.gz
HUVEC	GSM958734	wgEncodeCaltechRnaSeqHuvecR2x75I1200TSSRep2V3.gtf.gz
NHEK	GSM958736	wgEncodeCaltechRnaSeqNhekR2x75I1200TSSRep1V3.gtf.gz

Continued on next page

Continued from previous page

Cell type	GEO Accession	File URL suffix
NHEK	GSM958736	wgEncodeCa1techRnaSeqNhekR2x75I1200TSSRep2V3.gtf.gz
NHLF	GSM958746	wgEncodeCa1techRnaSeqNh1fR2x75I1200TSSRep1V3.gtf.gz
NHLF	GSM958746	wgEncodeCa1techRnaSeqNh1fR2x75I1200TSSRep2V3.gtf.gz

1507

1508 ***Mus musculus* source data of ChIP-seq on histone H3 modifications (SRA**
 1509 **files) [80, 78]**

1510 For downloading, the URL must be constructed by adding the following prefix to each file listed:

1511

1512 `ftp://ftp-trace.ncbi.nlm.nih.gov/sra/sra-instant/reads/ByRun/sra/SRR/`

Cell type	Antibody	Rep #	GEO Accession	File URL suffix
E14	IgG	1	GSM881345	SRR414/SRR414932/SRR414932.sra
E14-day0	H3K27ac	1	GSM881349	SRR414/SRR414936/SRR414936.sra
E14-day0	H3K27me3	1	GSM881350	SRR414/SRR414937/SRR414937.sra
E14-day0	H3K36me3	1	GSM881351	SRR414/SRR414938/SRR414938.sra
E14-day0	H3K4me1	1	GSM881352	SRR414/SRR414939/SRR414939.sra
E14-day0	H3K4me3	1	GSM881354	SRR414/SRR414941/SRR414941.sra
E14-day4	H3K27ac	1	GSM881357	SRR414/SRR414945/SRR414945.sra
E14-day4	H3K27me3	1	GSM881358	SRR414/SRR414946/SRR414946.sra
E14-day4	H3K36me3	1	GSM881359	SRR414/SRR414947/SRR414947.sra
E14-day4	H3K4me1	1	GSM881360	SRR414/SRR414948/SRR414948.sra
E14-day4	H3K4me3	1	GSM881362	SRR414/SRR414950/SRR414950.sra
E14-day6	H3K27ac	1	GSM881366	SRR414/SRR414955/SRR414955.sra
E14-day6	H3K27me3	1	GSM881367	SRR414/SRR414956/SRR414956.sra
E14-day6	H3K36me3	1	GSM881368	SRR414/SRR414957/SRR414957.sra
E14-day6	H3K4me1	1	GSM881369	SRR414/SRR414958/SRR414958.sra
E14-day6	H3K4me3	1	GSM881371	SRR414/SRR414960/SRR414960.sra
Heart (8 wks/o)	H3K27ac	1	GSM1000093	SRR566/SRR566827/SRR566827.sra
Heart (8 wks/o)	H3K27ac	2	GSM1000093	SRR566/SRR566828/SRR566828.sra
Heart (8 wks/o)	H3K27me3	1	GSM1000131	SRR566/SRR566903/SRR566903.sra
Heart (8 wks/o)	H3K27me3	2	GSM1000131	SRR566/SRR566904/SRR566904.sra
Heart (8 wks/o)	H3K36me3	1	GSM1000130	SRR566/SRR566901/SRR566901.sra
Heart (8 wks/o)	H3K36me3	2	GSM1000130	SRR566/SRR566902/SRR566902.sra
Heart (8 wks/o)	H3K4me1	1	GSM769025	SRR317/SRR317255/SRR317255.sra
Heart (8 wks/o)	H3K4me1	2	GSM769025	SRR317/SRR317256/SRR317256.sra
Heart (8 wks/o)	H3K4me3	1	GSM769017	SRR317/SRR317239/SRR317239.sra
Heart (8 wks/o)	H3K4me3	2	GSM769017	SRR317/SRR317240/SRR317240.sra
Heart (8 wks/o)	Input	1	GSM769032	SRR317/SRR317269/SRR317269.sra
Heart (8 wks/o)	Input	2	GSM769032	SRR317/SRR317270/SRR317270.sra
Liver (8 wks/o)	H3K27ac	1	GSM1000140	SRR566/SRR566921/SRR566921.sra
Liver (8 wks/o)	H3K27ac	2	GSM1000140	SRR566/SRR566922/SRR566922.sra
Liver (8 wks/o)	H3K27me3	1	GSM1000150	SRR566/SRR566941/SRR566941.sra
Liver (8 wks/o)	H3K27me3	2	GSM1000150	SRR566/SRR566942/SRR566942.sra
Liver (8 wks/o)	H3K36me3	1	GSM1000151	SRR566/SRR566943/SRR566943.sra
Liver (8 wks/o)	H3K36me3	2	GSM1000151	SRR566/SRR566944/SRR566944.sra

Continued on next page

Continued from previous page

Cell type	Antibody	Rep #	GEO Accession	File URL suffix
Liver (8 wks/o)	H3K4me1	1	GSM769015	SRR317/SRR317235/SRR317235.sra
Liver (8 wks/o)	H3K4me1	2	GSM769015	SRR317/SRR317236/SRR317236.sra
Liver (8 wks/o)	H3K4me3	1	GSM769014	SRR317/SRR317233/SRR317233.sra
Liver (8 wks/o)	H3K4me3	2	GSM769014	SRR317/SRR317234/SRR317234.sra
Liver (8 wks/o)	Input	1	GSM769034	SRR317/SRR317273/SRR317273.sra
Liver (8 wks/o)	Input	2	GSM769034	SRR317/SRR317274/SRR317274.sra

1513

1514 ***Mus musculus* RNA-seq source data (BAM files) [80, 78]**

1515 For downloading, the URL must be constructed by adding one of the two following prefixes to
1516 each file listed:

- 1517 1. <ftp://ftp.ncbi.nlm.nih.gov/geo/samples/GSM881nnn/>
1518 2. <ftp://hgdownload.cse.ucsc.edu/goldenPath/mm9/encodeDCC/wgEncodeLicrRnaSeq/>

Cell type	Rep #	GEO Accession	File URL suffix
E14-day0	1	GSM881355	[<i>prefix_1</i>]GSM881355/supp1/GSM881355_E14_RNA.bam.gz
E14-day4	1	GSM881364	[<i>prefix_1</i>]GSM881364/supp1/GSM881364_E14_RNA_d4.bam.gz
E14-day6	1	GSM881373	[<i>prefix_1</i>]GSM881373/supp1/GSM881373_E14_RNA_d6.bam.gz
Heart (8 wks/o)	1	GSM929707	[<i>prefix_2</i>]wgEncodeLicrRnaSeqHeartCell1PapMAdult8wksC57b16A1nRep1.bam
Heart (8 wks/o)	2	GSM929707	[<i>prefix_2</i>]wgEncodeLicrRnaSeqHeartCell1PapMAdult8wksC57b16A1nRep2.bam
Liver (8 wks/o)	1	GSM929711	[<i>prefix_2</i>]wgEncodeLicrRnaSeqLiverCell1PapMAdult8wksC57b16A1nRep1.bam
Liver (8 wks/o)	2	GSM929711	[<i>prefix_2</i>]wgEncodeLicrRnaSeqLiverCell1PapMAdult8wksC57b16A1nRep2.bam

1519

1520 ***Drosophila melanogaster* source data of ChIP-seq on histone H3
1521 modifications (SRA files) [74, 76]**

1522 For downloading, the URL must be constructed by adding the following prefix to each file listed:

- 1523
1524 <ftp://ftp-trace.ncbi.nlm.nih.gov/sra/sra-instant/reads/ByRun/sra/SRR/SRR030/>

Developmental time point/period	Antibody	GEO Accession	File URL suffix
0-4h embryos	H3K27ac	GSM401407	SRR030295/SRR030295.sra
0-4h embryos	H3K27me3	GSM439448	SRR030360/SRR030360.sra
0-4h embryos	H3K4me1	GSM401409	SRR030297/SRR030297.sra
0-4h embryos	H3K4me3	GSM400656	SRR030269/SRR030269.sra
0-4h embryos	H3K9ac	GSM401408	SRR030296/SRR030296.sra
0-4h embryos	H3K9me3	GSM439457	SRR030369/SRR030369.sra
0-4h embryos	Input	GSM400657	SRR030270/SRR030270.sra
4-8h embryos	H3K27ac	GSM401404	SRR030292/SRR030292.sra

Continued on next page

Continued from previous page

Developmental time point/period	Antibody	GEO Accession	File URL suffix
4-8h embryos	H3K27me3	GSM439447	SRR030359/SRR030359.sra
4-8h embryos	H3K4me1	GSM401406	SRR030294/SRR030294.sra
4-8h embryos	H3K4me3	GSM400674	SRR030287/SRR030287.sra
4-8h embryos	H3K9ac	GSM401405	SRR030293/SRR030293.sra
4-8h embryos	H3K9me3	GSM439456	SRR030368/SRR030368.sra
4-8h embryos	Input	GSM400675	SRR030288/SRR030288.sra
8-12h embryos	H3K27ac	GSM432583	SRR030332/SRR030332.sra
8-12h embryos	H3K27me3	GSM439446	SRR030358/SRR030358.sra
8-12h embryos	H3K4me1	GSM432593	SRR030342/SRR030342.sra
8-12h embryos	H3K4me3	GSM432585	SRR030334/SRR030334.sra
8-12h embryos	H3K9ac	GSM432592	SRR030341/SRR030341.sra
8-12h embryos	H3K9me3	GSM439455	SRR030367/SRR030367.sra
8-12h embryos	Input	GSM432636	SRR030346/SRR030346.sra
12-16h embryos	H3K27ac	GSM432582	SRR030331/SRR030331.sra
12-16h embryos	H3K27me3	GSM439445	SRR030357/SRR030357.sra
12-16h embryos	H3K4me1	GSM432591	SRR030340/SRR030340.sra
12-16h embryos	H3K4me3	GSM432580	SRR030329/SRR030329.sra
12-16h embryos	H3K9ac	GSM439458	SRR030370/SRR030370.sra
12-16h embryos	H3K9me3	GSM439454	SRR030366/SRR030366.sra
12-16h embryos	Input	GSM432634	SRR030344/SRR030344.sra
16-20h embryos	H3K27ac	GSM401401	SRR030289/SRR030289.sra
16-20h embryos	H3K27me3	GSM439444	SRR030356/SRR030356.sra
16-20h embryos	H3K4me1	GSM401403	SRR030291/SRR030291.sra
16-20h embryos	H3K4me3	GSM400658	SRR030271/SRR030271.sra
16-20h embryos	H3K9ac	GSM401402	SRR030290/SRR030290.sra
16-20h embryos	H3K9me3	GSM439453	SRR030365/SRR030365.sra
16-20h embryos	Input	GSM400659	SRR030272/SRR030272.sra
20-24h embryos	H3K27ac	GSM401423	SRR030311/SRR030311.sra
20-24h embryos	H3K27me3	GSM439443	SRR030355/SRR030355.sra
20-24h embryos	H3K4me1	GSM439464	SRR030376/SRR030376.sra
20-24h embryos	H3K4me3	GSM400672	SRR030285/SRR030285.sra
20-24h embryos	H3K9ac	GSM401424	SRR030312/SRR030312.sra
20-24h embryos	H3K9me3	GSM439452	SRR030364/SRR030364.sra
20-24h embryos	Input	GSM400673	SRR030286/SRR030286.sra
L1 larvae	H3K27ac	GSM432581	SRR030330/SRR030330.sra
L1 larvae	H3K27me3	GSM439442	SRR030354/SRR030354.sra
L1 larvae	H3K4me1	GSM432588	SRR030337/SRR030337.sra
L1 larvae	H3K4me3	GSM400662	SRR030275/SRR030275.sra
L1 larvae	H3K9ac	GSM401422	SRR030310/SRR030310.sra
L1 larvae	H3K9me3	GSM439451	SRR030363/SRR030363.sra
L1 larvae	Input	GSM400663	SRR030276/SRR030276.sra
L2 larvae	H3K27ac	GSM401419	SRR030307/SRR030307.sra
L2 larvae	H3K27me3	GSM439441	SRR030353/SRR030353.sra
L2 larvae	H3K4me1	GSM401421	SRR030309/SRR030309.sra
L2 larvae	H3K4me3	GSM400668	SRR030281/SRR030281.sra
L2 larvae	H3K9ac	GSM401420	SRR030308/SRR030308.sra
L2 larvae	H3K9me3	GSM439450	SRR030362/SRR030362.sra
L2 larvae	Input	GSM400669	SRR030282/SRR030282.sra
Pupae	H3K27ac	GSM401413	SRR030301/SRR030301.sra
Pupae	H3K27me3	GSM439439	SRR030351/SRR030351.sra
Pupae	H3K4me1	GSM401415	SRR030303/SRR030303.sra

Continued on next page

Continued from previous page

Developmental time point/period	Antibody	GEO Accession	File URL suffix
Pupae	H3K4me3	GSM400664	SRR030277/SRR030277.sra
Pupae	H3K9ac	GSM401414	SRR030302/SRR030302.sra
Pupae	H3K9me3	GSM439449	SRR030361/SRR030361.sra
Pupae	Input	GSM400665	SRR030278/SRR030278.sra

1525

1526 ***Drosophila melanogaster* RNA-seq source data (SAM files) [74, 76]**

1527 For downloading, the URL must be constructed by adding the following prefix to each file listed:

1528

1529 `ftp://data.modencode.org/all_files/dmel-signal-1/`

Developmental time point/period	GEO Accession	File URL suffix
0-4h embryos	GSM451806	2010_0-4_accepted_hits.sam.gz
4-8h embryos	GSM451809	2019_4-8_accepted_hits.sam.gz
8-12h embryos	GSM451808	2020_8-12_accepted_hits.sam.gz
12-16h embryos	GSM451803	2021_12-16_accepted_hits.sam.gz
16-20h embryos	GSM451807	2022_16-20_accepted_hits.sam.gz
20-24h embryos	GSM451810	2023_20-24_accepted_hits.sam.gz
L1 larvae	GSM451811	2024_L1_accepted_hits.sam.gz
L2 larvae	GSM453867	2025_L2_accepted_hits.sam.gz
Pupae	GSM451813	2030_Pupae_accepted_hits.sam.gz

1530